A Technique for Image Quality Assessment

by

NS Ayesha Siddique

Supervisor

Col Abdul Ghafoor, PhD

A thesis submitted to the faculty of Electrical Engineering Department Military College of Signals, National University of Sciences and Technology, Rawalpindi as part of the requirements for the degree of MS in Electrical Engineering

JULY 2018

ABSTRACT

With the advancement field of imaging and multimedia tools and applications, photosensitive information presented by images is the foremost source of knowledge acquirement. In the practice of photosensitive information acquirement, storage, handling and transmission, some antiquity and noise can be acquainted with images that can damage photosensitive quality of the images. Usually, in digital imaging system, images are captured and converted into digital signal with the help of different sensors. This unprocessed signal of digital image signal is then handled to reduce noise and then compressed for the storage or transmission. When the end user finally observes the image, it can be different from the original form due to its exposure to innumerable varieties of distortions.

Image fusion is an advantageous job in image and video enrichment practices. It is very necessary to state the proper standard for the quality assessment of fused images on the origin of subjective analysis. Existing models and techniques for image quality assessment are not very competent for all sorts of images and operational conditions specifically for images of moving entities, remote sensing constraints and medical applications.

The research aims to propose image quality assessment technique with the objectives to assess the quality of images with subjective data analysis along with the inclusion of contrast, structural similarity and luminance and to improve the quality measure for images of all environments and exposures.

Image fusion is grouping of more than two or two images acquired with different sensors or functioning conditions to craft the efficient outcome in one image. This work focuses on a novel quality assessment technique for multi -exposure fused images in image fusion specifically and in general.

Declaration

I certify that the work *"A Technique for Image Quality Assessment"* exhibited in this thesis has not been submitted in support of any other award or educational qualification either at this institution or elsewhere.

Acknowledgements

All praises to Almighty ALLAH who showered his blessing and able me to complete such exploration work.

I would especially like to thank for an amazing support that my supervisors Col Abdul Ghafoor, PhD and Dr. Muhammad Mohsin Riaz have been, throughout the course of my thesis. They helped me a lot to able me in completing my MS Degree, they were all time readily available for guidance and to help me throughout my thesis.

Lastly, I would like to show gratitude to my mother (Mrs. Naila Siddique), father (Mr. Muhammad Siddique) and sister (Aleena Siddique) for all their care, love and support through my times of stress and excitement.

Dedication

I dedicate my work to,

my mother who always encouraged my higher education, for her prayers, love and motivation and sacrifices all along.

my supervisors and friends for their support and patience during all the phases of my MS

.

Table of Contents

List of Tables

List of Figures

Chapter 1

1. INTRODUCTION

Image quality states the quantity of degradation existing in an image and an image with superior quality is always anticipated. For instance, the images acquired with the camera can contain fluctuating quality. There is always the probability of the presence of noise or distortion in an image. These types of distortions can induced in the image because of different reasons including the acquisition of image, compression, decompression, storing of an image, and movement of the camera during capturing the image or accumulation of noise in an image. Image quality cannot be obtained with just observing the few parameters such as contrast, sharpness or brightness. A sharp image can contain salt and pepper noise. There is the strong requirement of the standardize process to assess the image quality irrespective of the category of distortion which has affected the quality of image.

Visual observations are extraordinarily important for human beings. Humans resolve numerous everyday matters, achieve a lot of information, and charm their selves thanks to their visualization. Human visual system (HVS) is a tremendously progressed part of the human nervous system which comprehends the data available in real time from the visible light to badge them to observe the real time videos and images. Even though the complex HVS which establishes significant part of the brain outstandingly transmits the optical tasks, it has explicit features, sometimes mentioned as HVS limits. Since productions of the digital image processing and computer graphics approaches are perceived by human matters, like approaches have to imitate the structures of HVS to produce perceptually precise and reasonable images and to advance the presentation of images. The information of HVS typically takes the practice of mathematical simulations and these simulations can be combined at numerous areas of the image processing and computer graphics. The arenas

where the application of HVS simulations becomes predominantly are image quality calculation, color image to gray-scale conversions and high dynamic range tone mapping. In many applications, the optical data available in an image is lastly established by the human beings and it is instinctively sensible to give the scores to the image quality individually (by humans) [65, 66]. Nevertheless, in actual situations subjective image quality assessment (IQA) is luxurious and in maximum of the real time submissions implement the substitute choice called as objective image quality assessment. Nevertheless, there are plentiful Objective IQA methods in digital image processing which could be categorized in numerous means. For instance, data metrics known as MSE and PSNR uses the fidelity of image and overlooks the graphical data. However, on the other side image metrics reflect the graphical evidence available in the image [67]. In accumulation to these two kinds of metrics, there are some objective metrics that reflect the reference data in computing the quality of image. These types of metrics can be full- references (FR), no-reference (NR) and reduced reference (RR) approaches.

1.1. Image Quality Assessment

The main objective of Image Quality Assessment (IQA) is to intelligently expect the human observations of the image quality. It is recognized that traditional metrics like the Root Mean Squared (RMS) error are not satisfactory for the comparison of images as they badly calculate the dissimilarities among the images as professed by human spectator. To resolve the difficulty correctly, numerous perceptual Image Quality Metrics have been offered. These metrics conventionally include a mathematical and logical HVS prototype to appropriately forecast the image dissimilarity as a human would observe it.

The assessment of image quality is very applied in numerous imaging uses. The leading areas of IQA get in the parts of observing the quality of images (e.g. in lossy image firmness), benchmarking of imaging uses, and enhancing the procedures and their constraint

backgrounds. Though, image quality metrics have positively been functional also to the image database recoveries, to the assessment of the perceptual influence of the different version of processes, to the perception-directed interpretation of moving picture, etc. However, it is significant to evaluate the fused image quality in advance for numerous applications and purposes like for medical diagnostics and remote sensing. With the purpose to assess the fused image quality, several scholars presented the numerous metrics to find the image quality for both quantitative and qualitative image analyses of images.

Qualitative analysis finds out the worth of fused image by evaluating the image visually while observing the both fused and input images. Quantitative analysis finds out the worth of the fused image by using two variations with and without the reference image. In case of reference image, quality of the fused image is assessed with metrics like root mean square error and mutual information, etc. Whereas without, in the case of absence of reference image, the quality/worth of fused image is calculated by metrics such as entropy and standard deviation, etc.

1.2. Problem Statement and Objectives

All of the existing image quality assessment techniques offer the quality scores which are quite near to the genuine quality of image but still not the precise quality. Existing techniques are distortion specific but a procedure should be comprehensive but and should be workable for all kinds of distortions.

The main objective of this thesis is to assess the quality of images with subjective data analysis along with the inclusion of contrast, structural similarity and luminance and to improve the quality measure for images of all environments and exposures.

1.3. Contributions

Contributions of thesis are conceded as:

- An efficient technique for image quality assessment working efficiently on all type of fused images.
- Addressing the problems and failure cases in existing techniques.

1.4. Thesis Outline

- Chapter 1: This chapter contains introduction and objectives. It also contains the contributions have been made in this chapter. This chapter is focusing on the significance of image quality assessment and its applications. The main aim to have the standardized image quality assessment that should closely similar to the human visual system. This chapter is briefly explaining the requirement and importance of an image quality assessment technique.
- Chapter 2: In this chapter, review of literature and background is given along with brief description of existing technique and quantitative measures used in this thesis. It is briefly explaining the advantages, uses and drawbacks of all the existing image assessment techniques. With the brief summary of existing methods to evaluate the image quality assessment, this chapter is also explaining that why still there is the strong requirement of a standardized image quality assessment technique.
- Chapter 3: This chapter deals with the techniques of image fusion that have been used for fusing the images. In this thesis, two types of existing image fusion techniques have been used to get the two sets of images acquired by fusing the multi-images with different techniques to find out the image quality assessment of images and compare them with the human observation.
- Chapter 4: This chapter deals with the brief explanation of the latest existing image quality assessment technique, finds and explains the failure cases of the existing technique by comparing and observing the results of the image quality assessment visually. After finding out the failure cases of the existing techniques, this chapter is

explaining the new technique being proposed for the image quality assessment and its algorithms briefly.

- Chapter 5: This chapter deals with experimental results and evaluation based on qualitative and quantitative comparisons with existing technique are provided. Furthermore, this chapter is presenting the results of the new technique with the help of 10 examples and comparing the values of the image quality assessment technique with the existing technique.
- Chapter 6: This chapter concludes the report and future work is proposed. This chapter highlights that still there is the space of new research and works in this field of image quality assessment and also proposes the new ideas and approaches to work on them.

Chapter 2

2. PRELIMINARIES

2.1. Literature Review

In the last few years, various researches presented different types of mathematical prototypes and different methods to examine the images and to evaluate the quality of image. In this thesis, different techniques of image quality assessment have been presented along with their strong and weak points.

The main objective of multi-sensory fusion is to integrate image data acquired from various sensors into a single data set. Multi-sensor image fusion is expedient and cost-effective than making the sensor with both resolution features. Medical images acquired from different sensors offer correspondent and conclusive information and few applications need incorporation of such information of images to get the effective outcome. Doctors get structural information by using the physical data and Magnetic Resonance Imaging (MRI) from Photon Emission Tomography (PET). Image fusion can produce a single combined image from various modality images of the similar subject and offer complete data for more investigation and diagnosis. But before fusion, it is compulsory to align source images precisely. Earlier then fusing images, it is necessary to retain all features present in the images and should not bring together any artifacts or variation which would confuse the viewer. Image quality assessment shows a significant role in medical uses.

The fused image quality is significant, as a Pan-sharpening practice adds the indicators into the image of the large spectral resolution from the large spatial resolution in order to get one output image with the large spatial and spectral resolution [14]. Different Image quality metrics are being used to scale different image processing techniques by matching the objective metrics. There are two types of metrics that is subjective and objective used to assess image quality.

2.1.1 Subjective techniques

Subjective quality assessment techniques are centered on the manual human findings and therefore turns out to be the tedious, time intense and does not supports and adds the computerization to the images [11]. These methods are suitable for images which are at the end of the day to be observed by humans, the technique being used for the computation of graphical image quality by subjective assessment. Nevertheless because of the weaknesses, they couldn't be effortlessly implemented for innumerable situations such as factual scenarios and problematic to be incorporated in the programmed schemes [9].

In subjective quality evaluation, images are delivered to a many observers and are requested to compare the original source images with distorted images to assess the quality of distorted images[38]. Afterwards, Mean opinion score (MOS) is calculated centered on evaluation of observers, which is considered as the image quality index. All images are presented to the viewers which are requested to score the images with the scale from one (1) to five (5). There are three diverse features used including the luminance, spotting distance between the spectator and display of the image and display characteristics are occupied into account while showing the subjective quality test [12].

a. Single Stimulus (SS) Method

This technique is used for assessing the Image Quality Algorithms (IQA) [22, 23] i.e. here a set of stimuli is occupied one at a time and contains a reference image in that set and not briefed to the viewer. Observer assesses the quality and score stated in a mathematical category assessment. Single finding is necessary per valuation and then the average score has been computed. The quality range will be extending over by the stimuli. But this technique encourages variation so other technique known as quality ruler method was analyzed.

b. Quality Ruler (QR) Technique

This technique contains a sequence of reference images whose scales are previously acknowledged and are closely spread out in quality, but extent an extensive range of quality collected[33]. It identifies the quality difference among them and the spectator discerns reference image adjacent to eminence to test stimulus by graphic toning and quality score is observed. As compare to the Single Stimulus (SS) technique it is more reliable and QR scores are exceedingly simultaneous to objective measure of falsifications than the SS scores [24].

c. Mean Opinion Score Technique

Mean opinion score method yield the precise results with slight number of scores. It is created by calculating the average of the outcomes of a set of standard and subjective test and turn as a display for the observed image quality [25, 26]. Score classes are shown in Table 2.1.

Table 2.1: Mean Opinion Score Classes

1	2	3	4	5
Very Poor Quality	Poor Quality	Good Quality	Very Good Quality'	Excellent Quality

The other techniques used are force-choice technique but it does not express the dissimilarity among the quality of images where in pairwise comparison judgment technique the quality difference among the two images are distinguished [27]. Drawbacks of subjective assessment include time consuming and are problematic to design and cannot be accomplished in real time [16]. Subjective assessment is not applicable for real-time processing since the test has to be performed with great care in order to obtain meaningful results. Moreover, it is not feasible to have human intervention with in-loop and on-service processes [75].

d. PSNR Metrics based on Human Visual System

This quality metrics uses the contrast sensitivity function and between-coefficient contrast masking of the DCT basis operations[34]. It has been revealed that the PSNR metrics overtakes the other available famous reference centered quality metrics and revealed the great correlation with the consequences of the subjective trials [77].

e. VSNR Metrics Based on Human Visual System

This metrics is calculated by the two-stage method [78]. In first step, contrast thresholds are computed for finding the distortions in the existence of original images by using the wavelet-centered prototypes of optical masking and optical synopsis to decide that whether the distortions in distorted image are observable or not. If the available distortions are under the inception point of recognition, the distorted image is appealed to be of the impeccable pictorial quality [48]. However, If the distortions in the image are more as compared to the benchmark value, a second step is functional, which functions centered on the pictorial property of the apparent contrast and worldwide preference. These two possessions are demonstrated as the Euclidean distances in the distortion contrast universe of multi-scale wavelet decay, and the final VSNR metric is achieved constructed on the modest linear synopsis of these spaces[40].

Nevertheless, the human visual system is a multifaceted and extremely nonlinear scheme, and best prototypes so far are only centered on the linear operators or the quasi-linear operators [75].

2.1.2 Objective Techniques

This technique is based on the quantitative approach according to which, strength, reference and distorted type of two different images are used to calculate an output in the form of number which predicts the quality of image. These objective quality based assessment techniques can be classified into full, reduced and no-reference.

a. No Reference Objective Technique

In no reference (NR) objective technique, in common the human optical system has no need of reference image or model to gauge the quality score of the output image under observation. This procedure is also known as the “blind models” approaches [12]. NR technique can be used in number of applications where quality evaluation is essential since they have no requisite of any reference image.

Numbers of the blind image quality valuation are distortion explicit. BLIINDS index is a no reference method and is used to calculate image quality constructed by removing the information of coefficients of local discrete cosine transform and calculate its kurtosis. The amount of weakness and tail weight is then calculated as [16]. Each value is then calculated and the ensuing values are combined together to get the value of global image kurtosis [17]. The current NR method does not perform well in general since it judges the quality solely based on the distorted medium and without any reference available [75].Current No-Reference Image Quality Assessment (NR-IQA) procedures do not offer the précised excellence score of the images as none of the NR-IQA procedure have the value of correlation equal to 1 and the calculation time is also large that bounds its presentation in the real time schemes [42]. One more restraint of the available NR-IQA is that the procedures are distortion related i.e. the procedures give appropriate outcomes solitary if the procedure is qualified for the distortion existent in test image.

Table 2.2: No-Reference Image Quality Calculation Techniques

Name of Algorithm	Creator	Features Used	Reference Keys
BIQI [71]	A.K.Moorthy A.C Bovik	Wavelet Transform in 3 scales and 3 orientations	PSNR
DIIVINE [72]	A.K.Moorthy A.C Bovik	Wavelet Transform to obtain sub-band coefficients for statistical features	SSIM PSNR
BLIINDS [69]	M.A Saad A.C. Bovik C. Charrier	Discrete Cosine Transform based contrast & structure features	PSNR

BLLINDS-II [70]	M.A Saad A.C. Bovik C. Charrier	Model based Discrete Cosine Transform domain NSS features	SSIM PSNR
Visual Codebook [73]	Peng Ye D. Doermann	Gabor Filtering in 4 orientations and 5 frequencies	SSIM PSNR

Disadvantages of the techniques stated in table 2.2 are:

• These techniques are not completely no-reference techniques, a customary data set is mandatory to first sequence the technique for the explicit kind of distortions.

• Calculation time is too much; therefore it is not appropriate for the real time uses.

• Variance in the real Differential Mean Opinion Score (DMOS) and the quality score set by current techniques.

b. Reduced Reference Objective Technique

In this objective based technique, partial data concerning the 'impeccable form' is offered. A side-channel subsists where some data of reference can be obtainable for quality evaluation method. In this algorithm, this half reference data is used to calculate the worth of slanted signal of scene [10]. Reduced Reference metric requires a feature vector of reference source image to evaluate its quality. These vectors are the derivative of ‘m’ which represents the constraints of algebraic models as hidden in figure 2.1.

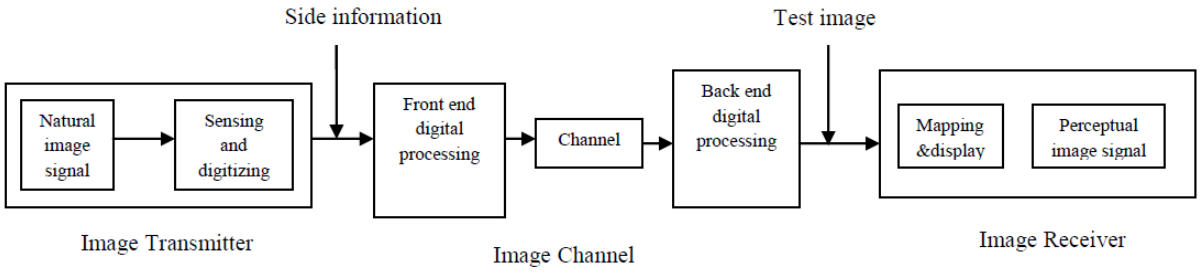

Figure 2.1: Reduced Reference Objective 1

The different methods used in Reduced Referenced Quality Assessment are primarily assembled on modeling of the image spins; subsequent is concentrated on HVS and the last one on NSS [18].

Concentrated on HVS technique, components are removed to intend an abridged explanation of the image that is not openly linked to any particular distortion scheme. Preparation for diverse types of distortion is required [19][20]. Irregularity will happen due to the distortions and is calculated centered on the natural image information and here preparation is not required for it and is further applicable to the graphic observation of image quality.

The arithmetical terminations among wavelet coefficients can be abridged by divisive normalization transform (DNT) and this is calculated by the GSM model [43]. Image quality can be assessed by equating the arithmetical features of group of reduced reference images dig out from the range of DNT depictions of original and the slanted images. The numerical properties are significantly altered under the diverse forms of image distortions [21].

Subsequently the removed partial reference data is much lighter as compare to the complete reference, thus the reduced-reference technique can be used for the distant location (For example., the transmit site and the receiving end of broadcast) with realistic bandwidth outlays to attain the improved consequences than the no-reference technique, or in a condition where a reference is existing like video encoder to decrease the calculation constraint (particularly in the frequent management and the optimization) [75].

c. Full Reference Objective Technique

In this objective full reference IQA technique, in common the human visual system needs a reference model to gage the image quality score [12]. In this technique, reference image is recognized and calculate the visual quality of image by paralleling the slanted signal with the original image being used for the reference. For this determination, peak signal to noise ratio (PSNR) and Mean Square error (MSE) and are being used generally [16][76].

In common, there are two classes for the objective based quality assessment technique comprising the simple statistic error metrics and human optical system feature centered metrics.

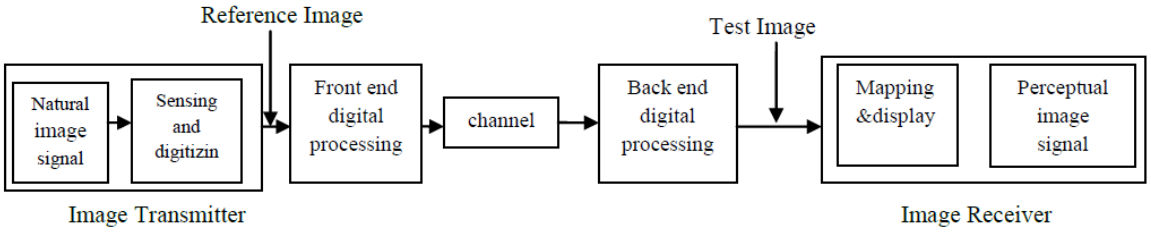

Figure 2.2: Full-reference Objective Tec 1

A. Simple Statistics Error Metrics

I. Simple Statistics Error Metrics

Measurement techniques reflect the human visual System (HVS) features to integrate with perceptual image quality. HVS uses the psychophysical quantities to calculate the image optical quality and then image is crumbled to acquire the gain control in sub-band crumbled domain [28] MSE is used to assess the image quality and is defined as:

$$MSE = \frac{1}{MXN}\sum_{i=1}^{N}\sum_{j=1}^{N}(a_{ij} - b_{ij})^2 \qquad (2.1)$$

In above equation, a is source image, b is the distorted image, M is representing the width and N is the height of image. By increasing the value of MSE compression ratio also increases. Pixel by pixel comparison of images become impeccable If MSE value declines to zero. MSE is a quite simpler one [16].

MSE do not use the structure or data structures of the original source image. Designs and roughness bring the bulk of the statistics in the original image [44]. Consequently, the pixels have robust spatially native dependences. Nevertheless, such appreciated evidence is overlooked by MSE [74].

II. Peak Signal to Noise Ratio (PSNR)

PSNR is a conventional index stated as proportion of extreme apparent power of signal and mortifying noise that aches the steadiness of its demonstration [12].

$$PSNR = 10.\, log_{10}\left(\frac{255^2}{MSE}\right)[db] \qquad (2.2)$$

In the above equation, 255 is utmost likely value of pixels of image where pixels are denoted by 8 bits for each sample [45].

Both MSE and PSNR are well-demarcated just for the luminance data; there is no covenant on the calculation of the values of color.

III. Average Difference:

This technique also named as AD calculates the average value of difference between the source and test image. It is given by the equation (2.3):

$$AD = \frac{1}{AB}\sum_{a=1}^{A}\sum_{b=1}^{B}(p(a,b) - q(a,b)) \qquad (2.3)$$

IV. Maximum Difference

This method is also called as MD which calculates the maximum value of the error signal i.e. (difference between the source and test image) [29]:

$$MD = MAX|p(a,b) - q(a,b)| \qquad (2.4)$$

V. Mean Absolute Error

MAE calculates the average value of complete discrepancy among the reference and test image. It is given by the equation (2.5):

$$MAE = \frac{1}{AB}\sum_{a=1}^{A}\sum_{b=1}^{B}|p(a,b) - q(a,b)| \qquad (2.5)$$

VI. Peak Mean Square Error:

PMSE can be calculated by:

$$PMSE = \frac{1}{AB}\ X\ \frac{\sum_{a=1}^{A}\sum_{b=1}^{B}(p(a,b)-q(a,b))^2}{(MAX\ (p(a,b))^2} \qquad (2.6)$$

The unassertive and best largely used evaluation of image quality full-reference based technique is the Mean Square Error and the Peak Signal to Noise Ratio. Profits of both include the quick and tranquil to execute [46]. However, it merely and quantitatively calculates the error signal. With PSNR, large values represent the higher image alikeness, whereas with the MSE, larger values represent the lower image alikeness [10].

The foremost restraint of the full-reference image quality calculation processes is that they need the source, factual image to assess the quality of the slanted image. These techniques cannot be castoff in the applications where the reference image does not exist. The PSNR values also do not dependable with HVS [68].

B. Human Visual System Feature Centered Metric:

I. SSIM:

Structural similarity index measure is a method for calculating the alikeness among two images [30]. It offers alteration/similarity map in the domain of pixels [32]. SSIM trails the calculation of structural data adaptation can deal a noble estimate to perceived image spin. SSIM links the native arrangements of values of the pixel intensity which are standardized like contrast and luminance. It is an upgraded form of customary approaches like MSE and PSNR. The SSIM index can be expressed with number flanked by 0 and 1[47] . Where, “0” represents the zero likeness with the source image, whereas 1 denotes the clear-cut alike image as the original. The amount of measure amid two windows together with a and b of common size (M×M) is specified as shadows:

$$SSIM(a,b) = \frac{\{(2\mu_a\mu_b+K_1)(2\sigma_{ab}+K_2)\}}{\{(\mu_a{}^2+\mu_b{}^2+K_1)(\sigma_a^2+\sigma_b^2+K_2)\}} \qquad (2.7)$$

In the above equation, μ_a is representing the average value of a, μ_b is representing the average value of b, σ_a and σ_b are demonstrating the standard deviation among source and

treated images pixels, correspondingly. $K_1$and K_2 are positive constants selected empirically to escape the uncertainty of measure. SSIM is stated in the form of a number amid -1 and +1[49].

Nevertheless, SSIM is only a distinct-scale technique and is not very active to evaluate the quality of the multi-fusion images. However, SSIM is delicate to the comparative conversions, revolutions, and scaling of the images [75].

II. Complex-wavelet SSIM

CW-SSIM is nearby calculated from every sub-band and then be an average of over the sub-bands and space, resilient an inclusive CW-SSIM index among the source image and the slanted images. This technique is vigorous with deference to the changes in the luminance, contrast and translations [79].

III. DSSIM

This compromises the structural divergence metrics which is derivated from SSIM as stated below:

$$DSSIM(a,b) = \frac{1}{(1-SSIM(a,b))} \qquad (2.8)$$

IV. MSSIM

Mean value of Structure Similarity Index Measure is named as mean structural similarity index metric (MSSIM) [31] and it is signified as:

$$MSSIM(A,B) = \frac{1}{N}\sum_{l=1}^{N} SSIM(al,bl) \qquad (2.9)$$

V. FSIM (FR, Signal feature extracted metric)

This technique is a freshly established image quality metric, which equates the feature sets with low-level among the original and distorted image centered on the point that the HVS comprehends an image generally rendering to its low-level structures. Phase congruency is

the main element to be castoff in the calculation of the FSIM. Gradient magnitude is the second element to be summed in the FSIM metric because phase congruency is the contrast invariant and contrast evidence also disturbs the human visual system insight of the image quality. Essentially, in FSIM index, the resemblance measures for the PC and GM all trail the similar method as in the SSIM metric [80][88].

SSIM is extensively used technique for the measurement of the image quality. It works precisely can calculate the improved through the distortion types than the MSE and PSNR, but miss the mark in case of extremely blurred image. The feature similarity (FSIM) index [148] appears to the one which can shatter the SSIM in numerous databases. But it still cannot achieve the accurate results as compare to the other existing quality metrics with deference to all types of image matters and distortion types [81].

Divergent image quality images have coarsely similar mean square error than original input image. This technique offers an improved presentation of image worth.

d. Few Recent Techniques of Image Quality Assessment

I. A Training-Based No-Reference Image Quality Assessment Algorithm

In this technique, a two-stage approach to evaluate the image quality has been used. In first stage, a face detection procedure has been used to perceive the human faces from image. In the second stage, the spectrum spreading of the identified area is equated with the qualified model to conclude its quality score for the image [82].

The constraint is that it mainly smears to the images that comprise human faces. Even though the creators of this technique stated that it’s not problematic to simplify the faces to the other substances, they still only delivered the consequences which have used the images that contains the human faces to demonstrate the practicality of their technique [83].

II. No-Reference Image Quality Assessment Using the Modified Extreme Learning Machine Classifier

In this technique, the use of machine learning has been proposed to calculate the visual excellence of the JPEG-coded images. Structures are removed by bearing in mind the features connected with the sensitivity of the human visual system like background luminance, edge length, background activity and edge amplitude. The pictorial quality of the image is then calculated by using the forecasted number of class and their assessed subsequent probability. It was revealed by the investigational consequences that the method achieves enhanced than other available metrics [84][85].

However, it is only relevant to the JPEG-coded images as the above mentioned structures are computed on the basis of the DCT blocks[83].

III. Calculation Based on the Support Vector Regression (SVD)

Narwaria and Lin [16] offered to use the singular vectors from the singular value decomposition as elements to enumerate the main essential information present in the images. Afterwards, they smeared the support vector regression for the calculation of the image quality, where the SVR technique has the capability to acquire the multifaceted data designs and maps convoluted structures into the appropriate score.

However this technique is constructed on machine learning and couldn't offer the real consequences for the images having the altered colors and backgrounds [86].

IV. Multi-method fusion (MMF) Image Quality Assessment Algorithm

It is inspired by the reflection that none of the single technique provides the best results in all circumstances. A regression method has been used to conglomerate the quality scores of the numerous IQA approaches in the MMF. Initially, a large amount of samples of images were gathered, each of them has the score categorized by the human spectators and scores related

with the numerous IQA techniques. This MMF quality score is then acquired by the non-linear grouping of the quality scores calculated with the manifold approaches (comprising the SSIM, FSIM, and so on) with appropriate weights found by a training procedure. To recover the forecasted scores additionally, slanted images are categorized into the five clusters centered on the different types of distortion, and reversion is achieved inside the each cluster, which is termed as the context-dependent MMF quality assessment technique (CD-MMF). Up to now, MMF deals as one of the finest IQA outcomes in numerous widespread databases like LIVE, CSIQ, and TID 2008 [83].

V. Block-based MMF

A block-based MMF [19] technique was also suggested for the image quality assessment. In the first step, an image is disintegrated into the small blocks. These small blocks are then categorized into the three types including (edge, smooth and texture), whereas distortions are then categorized into the other five groups. Lastly, one appropriate IQA metric is designated for every block centered on the type of the block and the distortion cluster. Combining over all the small blocks gives the ultimate quality score of the image. It deals with the reasonable performance with MMF for the database TID2008 [87].

VI. ParaBoost Technique

In this technique, initially few features were extracted from the existing image quality metrics and sequence them to custom the basic image quality scorers. Formerly, extra structures were extracted to discourse the explicit types of distortion and sequence them to create the auxiliary image quality scorers. Together BIQSs and AIQSs are accomplished on the subsets of the small image of convinced distortion types and, as a consequence, they are feeble players with admiration to an extensive diversity of the distortions. Lastly, ParaBoost

framework was adopted, which is an arithmetical scorer collection system for the SVR, to fuse the marks of BIQSs and AIQSs to assess the images comprising an extensive range of the distortion types. This ParaBoost procedure can be effortlessly protracted to the images of new distortion kinds. Wide trials are directed to validate the greater enactment of the ParaBoost technique, which overtakes all the available IQA approaches by an important boundary. Precisely, the Spearman rank order correlation coefficients of the ParaBoost technique with admiration to the TID2013, LIVE, CSIQ and TID2008, and image quality folders are 0.98, 0.97, 0.98, and 0.96, correspondingly [89].

Besides this most of the existing image fusion quality assessment techniques [1]-[4] are mainly based on structural similarity index which require a perfect reference image and are mostly inefficient. The work in [5], [6] use structure similarity theory to define the quality assessment measure; however these can only take a pair of images as the input. High-tech image quality assessment methods could not deliver satisfactory estimates of alleged quality of the fused images. The work in [7], [8] involves the entropy calculations of the intensity values of pixels and transform coefficients; nevertheless these techniques have deprived association with the perceptual image quality. The actual reason behind this can be that the quality of fused images is exceedingly content reliant on only entropy of the image strength histogram is inadequate in apprehending the perceptual spins lead by multi exposure image fusions. The work in [1]-[4] uses the native structure-conservation built models like SSIM and gradient centered methodologies, nevertheless they are repeatedly futile in taking the squalors of luminance steadiness crossways the image space. In summary the existing image fusion assessment techniques particularly for multi exposure image fusion lack in accuracy and flexibility.

Chapter 3

3. WORKING METHODOLOGY

In this, different data set of images has been used to fuse these images with two different techniques of image fusion. These fused images were tested by already available techniques of image quality assessment techniques.

3.1. Techniques Used for Image Fusion

i. Multi-focus Image Fusion Based on Wavelet Transform and Adaptive Block

In this fusion technique, blocks of different levels and sizes and amalgamates the adaptive size of the block. First of all, it divides the input sources images into the different blocks of 16 x 16 and then these blocks are the identified by using the block clarity algorithm [50]. After the complete examination of block clarity, these divided blocks of source images can be further divided in two different classes, the boundary and non-boundary blocks. Since, the non-boundary blocks were extracted from the corresponding source image and afterwards inserted in fused image. The boundary blocks are fused by applying the technique of boundary block fusion [63].

A. Block Clarity Algorithm

i. In block clarity technique, discrete wavelet transform is executed to find the wavelet coefficients for source blocks A and B of size (Q, Q) [63].

ii. In the second step, coefficients $aW_{detail}(p,q)$ and $bW_{detail}(p,q)$ of broad wavelet at level (1), for the input source blocks A and B are calculated; where detail = horizontal, diagonal and vertical [63].

iii. In the third step, native gradient of all the wavelet coefficients is then calculated as stated below:

$$G_1(W_{detail}(p,q) = \max\{maski * W_{detail}(p,q)| \, i = 1-8\} \qquad (3.1)$$

Where, the different eight masks are presented beneath [63]:

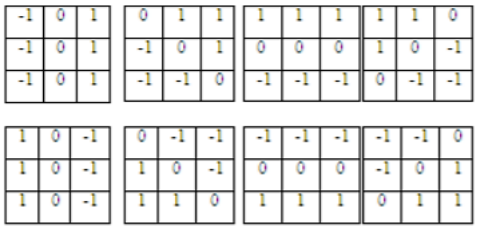

Figure 3.1 Eight Masks 1

iv. In the fourth step, level of activity of all wavelet coefficient is then calculated as mentioned below:

$$L\,(W_{detail}(p,q)=|\,W_{detail}(p,q)|+G_1W_{detail}(p,q) \qquad (3.2)$$

In the above equation, $L(W_{detail}(p,q))$ imitates the level of activity (L) of the wavelet coefficient $W_{detail}(p,q)$.

v. BCL of each block is then computed as mentioned below:

$$BCL=\sum_{detail}L\big(W_{detail}(p,q)\big) \qquad (3.3)$$

vi. Block of high BCL is deliberated as stronger [63].

B. Boundary Blocks Fusion Technique

i. In this technique, discrete wavelet transform is executed to find out the wavelet coefficients of source blocks A and B, with size (Q, Q).

ii. Wavelet coefficients $aW_{coef}(p,q)$ and $bW_{coef}(p,q)$ at level (5), for the source input blocks A and B are calculated; where coef symbolizes the horizontal, approximate, diagonal and vertical.

iii. In the third step, fused wavelet coefficients are calculated by finding the average of approximate source coefficients and then choosing the maximum comprehensive (vertical horizontal and diagonal) source image coefficients.

iv. In the last step, inverse discrete wavelet transform is calculated on the fused wavelet coefficients to find out the fused boundary block [63].

C. Results of Fusion

Input Images

Output Fused Image

Figure 3.2.1: Example#1

Input Images

Output Fused Image

Figure 3.2.2: Example#2

Input Images Output Fused Image

Figure 3.2.3: Example#3

Input Images Output Fused Image

Figure 3.2.4: Example#4

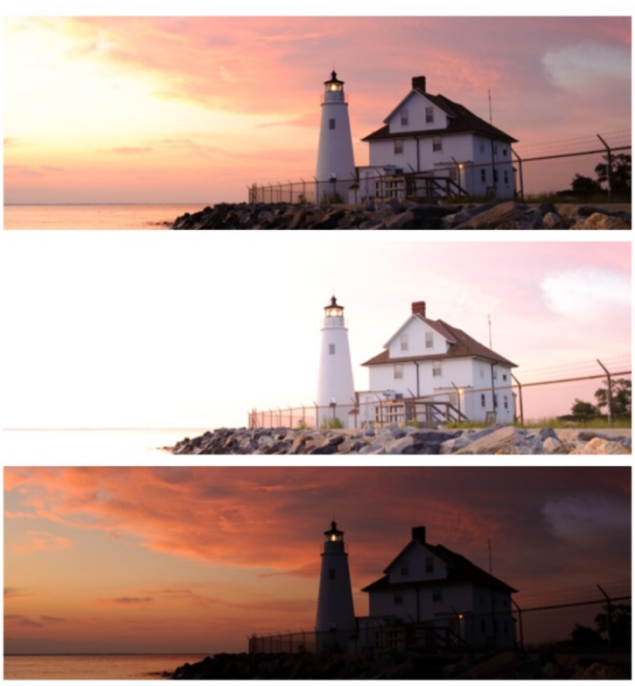

Input Images Output Fused Image

Figure 3.2.5: Example#5

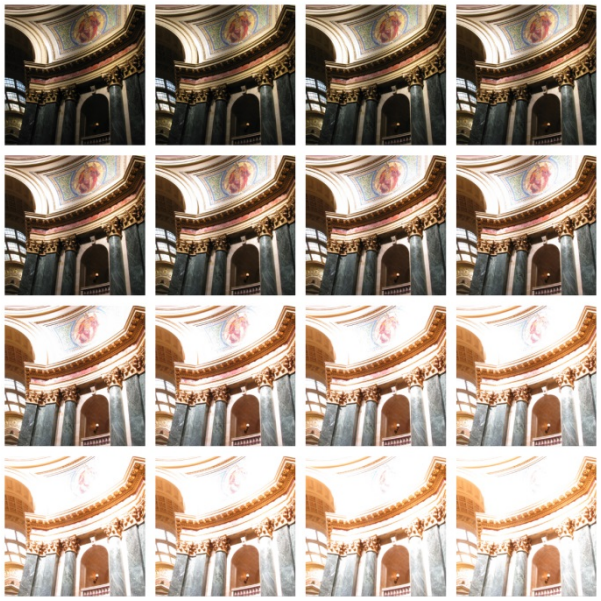

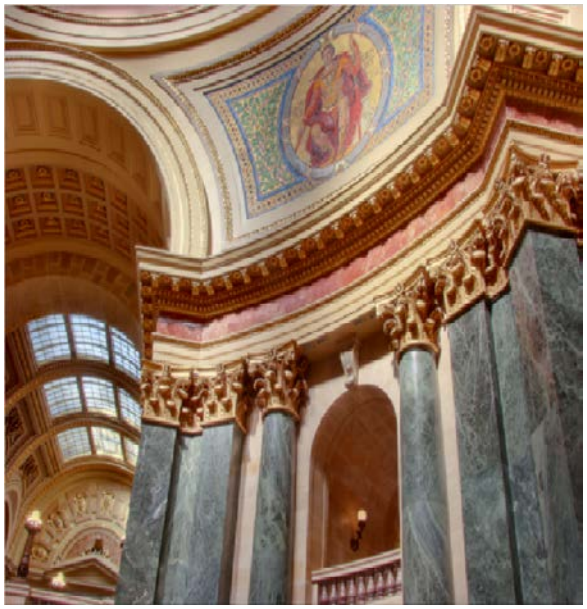

Input Images Output Fused Image

Figure 3.2.6: Example#6

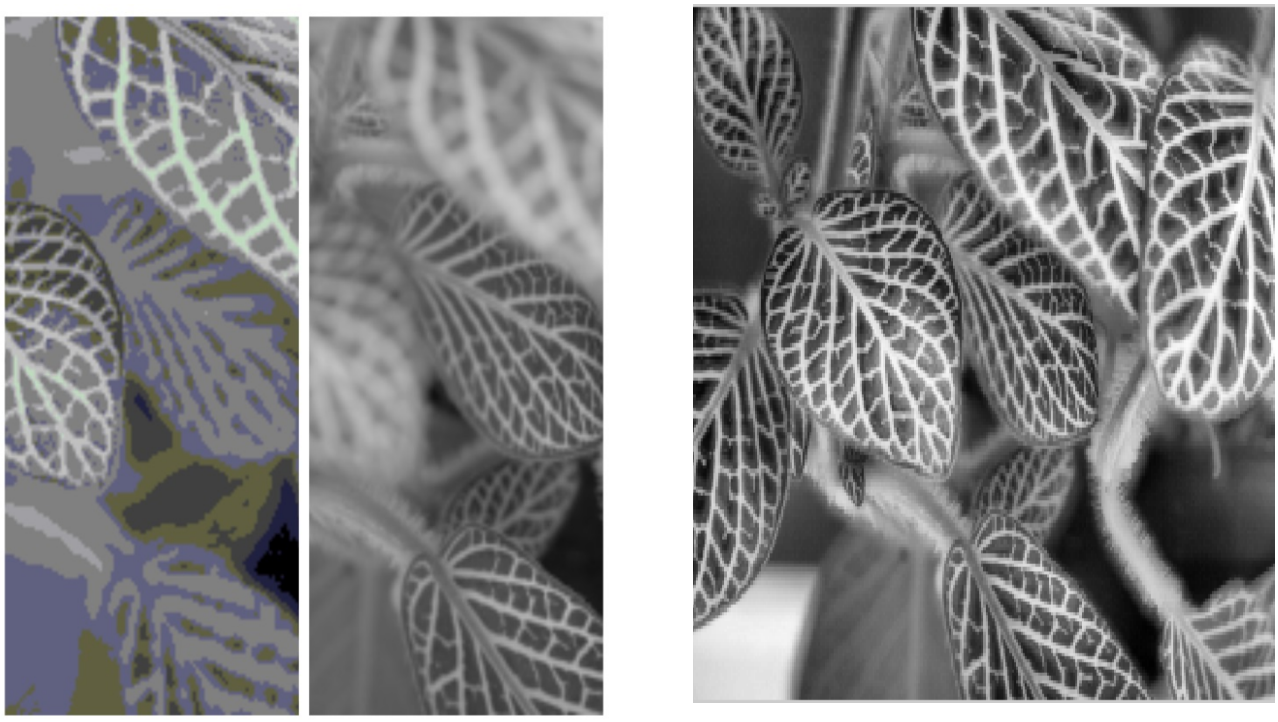

Input Images Output Fused Image

Figure 3.2.7: Example#7

Figure 3.2: Input Source Images and Fused Output Images For Algorithm 1

ii. Multi-scale Transform and Sparse Representation Image Fusion

In general, the Multi-scale transforms (MST) fusion approaches contain the below mentioned three steps [53].

- Decomposition of source images into the domain of a multi-scale transforms.
- Merging of the provided fusion rule with the transformed coefficients
- Lastly, reconstruction of the resultant fused image after finding the alike inverse transform above the pooled coefficients.

This method assumes that ultimate prominent data of input source images can be extracted from disintegrated image coefficients. Clearly, the assembly of transform region has the acute role in this technique [51].

In this technique, the original sparsity of the signals is reported by the sparse representation, which is absolutely related with the natural visual system of humans [54]. Behind this sparse

representation, the most basic assumption is that a signal (a ∈ Rn) can be easily portrayed and characterized by linear combination of "scarce" atoms with the help of an over-complete dictionary i.e. D ∈ Rn×p (q < p), in which q is representing the signal dimension whereas p is depicting the size of dictionary. According to this representation, the signal a can be demonstrated as a ≈ D_, I which _ ∈ Rm is unknown sparse coefficient vector. As dictionary is over-complete, this underdetermined system can be achieve by several solutions. The main aim of this sparse representation is to figure out the sparsest that contains the scarcest non-zero records between all the likely solutions which are recognized as the sparse coding [52]. The over-complete dictionary finds the sparse coding's capability of signal representation. Usually, two foremost classifications are available for offline methods to achieve the best dictionary results [39]. In the first approach, the investigative models like discrete cosine transform DCT and CVT are straightly used. On the other hand, this dictionary is limited to the different kind signals and cannot used for random signals. Second approach is to implement the machine learning system for acquiring the dictionary from large quantity of training image bits. With an assumption of √q×√q sized N training patches are reorganized in Rn space to column vectors, training database {bi} Ni=1 is created with each bi ∈ Rn. Therefore, this can be stated as:

$$D, \{a_i\}_{i=1}^{N} \min \sum_{i=1} \| _i \|_0 \quad s.t. \|b_i - Da_i\|_2 < \epsilon, i \in \{1, \ldots . N\}, \qquad (3.4)$$

In the above equation, " > 0" is representing the tolerance of error, {_i} Ni=1 is the unknown sparse vectors that is likely to {bi} Ni=1 and D ∈ Rq×p is the unused dictionary to be learned. The schematic illustration of fusion framework is presented in Fig. 3.4.
The comprehensive fusion technique encloses the below mentioned steps.

A. Multi-Scale Transforms (MST) Decomposition

Execution of MST on the two original source images$\{I_1, I_2\}$ to find out the high-pass bands represented as $\{H_1, H_2\}$and low-pass bands denoted as$\{L_1, L_2\}$.

B. Low-pass Fusion

(i) Implication of sliding window process for decomposing the $\{L_1, L_2\}$ into image patches starting at upper left and ending at the bottom right with length of r pixels. Assume that T number of patches are represented as:

$\{s_1^i\}_{i=1}^T$ *and* $\{s_2^i\}_{i=1}^T$ in $\{L_1, L_2\}$ correspondingly.

(ii) for each site denoted as i, reorder $\{s_1^i, s_2^i\}$ into the column vectors denoted as $\{v_A^i, v_B^i\}$ and then normalize the mean value of each vector to zero (0) to obtain the $\{\hat{v}_A^i, \hat{v}_{AB}^i\}$ by

$$\hat{v}_1^i = v_1^i - v_1^{-i}.1 \qquad (3.5)$$

$$\hat{v}_2^i = v_2^i - v_2^{-i}.1 \qquad (3.6)$$

In the above equations, 1 is representing the all-one valued vector of q × 1, here the v_1^{-i} and v_2^{-i} are denoting mean values of components in v_1^i and v_2^i correspondingly.

(ii) Computation of the sparse coefficient vector $\{\alpha_1^i, \alpha_2^i\}$s of $\{\hat{v}_1^i, \hat{v}_2^i\}$ by using the algorithm of orthogonal matching pursuit (OMP) by

$$\alpha_1^i = \arg\min_{\alpha} ||\alpha||_0 \quad s.t. \quad \left||\hat{v}_1^i - D\alpha\right|_2 < \epsilon \qquad (3.7)$$

$$\alpha_2^i = \arg\min ||\alpha||_0 \quad s.t. \quad \left||\hat{v}_2^i - D\alpha\right|_2 < \epsilon, \qquad (3.8)$$

In the above equations, D is the learned dictionary.

(iv) Merging the α_1^i and α_2^i with the rule of "max-L1" to get the fused sparse vector represented as:

$$\alpha_3^i = \begin{cases} \alpha_1^i & if \ \left\|\alpha_1^i\right\|_1 > \left\|\alpha_2^i\right\|_1 \\ \alpha_2^i & Otherwise \end{cases} \qquad (3.9)$$

The fused outcome of v_1^i and v_2^i is computed by

$$v_3^i = D\alpha_3^i + v_3^{-i}.1 \qquad (3.10)$$

In the above equation, the fused mean value v_3^{-i} is acquired by

$$v_3^{-i} = \begin{cases} v_1^{-i} \ \ if \ \ \alpha_3^i = \alpha_1^i \\ v_2^{-i} \qquad Otherwise \end{cases} \qquad (3.11)$$

(v) Repetition of the above mentioned process for all the patches of the source images in $\{s_1^i\}_{i=1}^T \ and \ \{s_2^i\}_{i=1}^T$ to get all fused vectors$\{v_3^i\}_{i=1}^T$. Let LF represents low-pass fused output. Forv_3^i, restructure it into s_3^i a patch and then plug s_3^i in to the input original situation inL_3. Since, patches are concurred; value of all pixels in L_3 is being an average of over its addition intervals.

C. High-pass Fusion

Fusion of $H_1 and \ H_2$ is accomplished to acquire H_f with extensive rule "-maximum-absolute" by extracting the absolute value of all coefficients as the calculation of the level of activity. In subsequent step, application of the consistency verification method is done to endorse that coefficient of fused image is not created from the other source input image by its most neighbors. It could be executed by using a minor bulk filter.

D. MST reconstruction

Perform the corresponding inverse MST over LF and HF to reconstruct the final fused image IF.

E. Results of Fusion

Input Images Output Fused Image

Figure 3.3.1: Example#1

Input Images Output Fused Image

Figure 3.3.2: Example#2

Input Images Output Fused Image

Figure 3.3.3: Example#3

Input Images Output Fused Image

Figure 3.3.4: Example#4

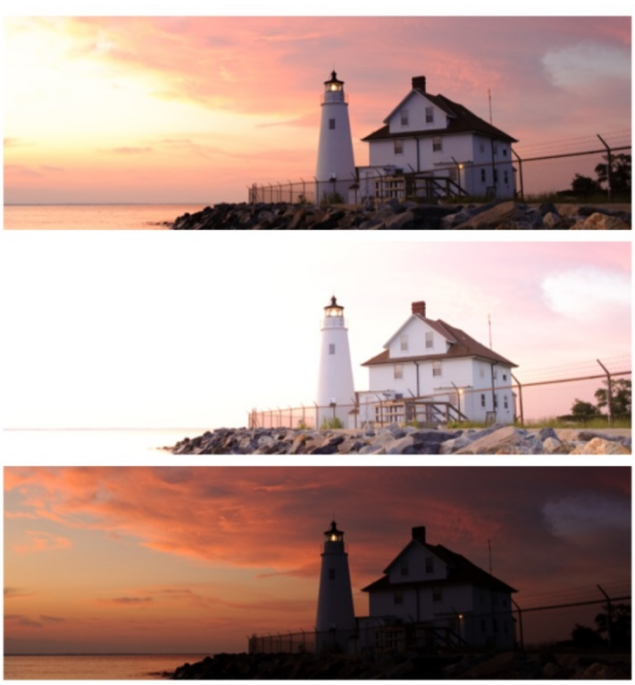

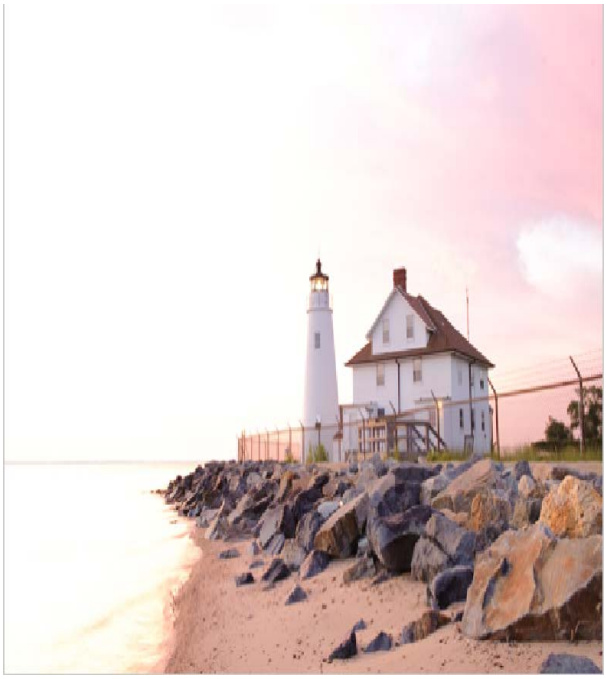

Input Images Output Fused Image

Figure 3.3.5: Example#5

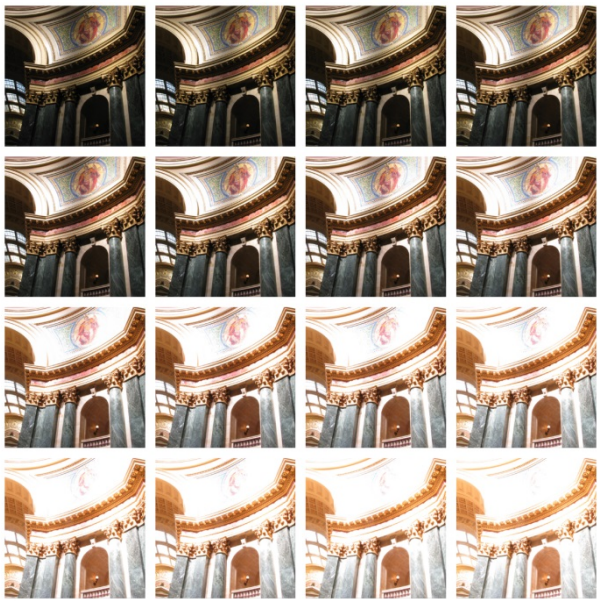

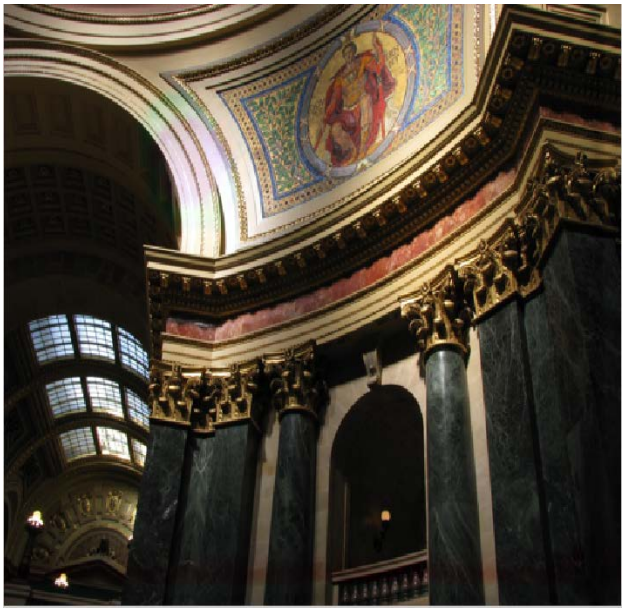

Input Images Output Fused Image

Figure 3.3.6: Example#6

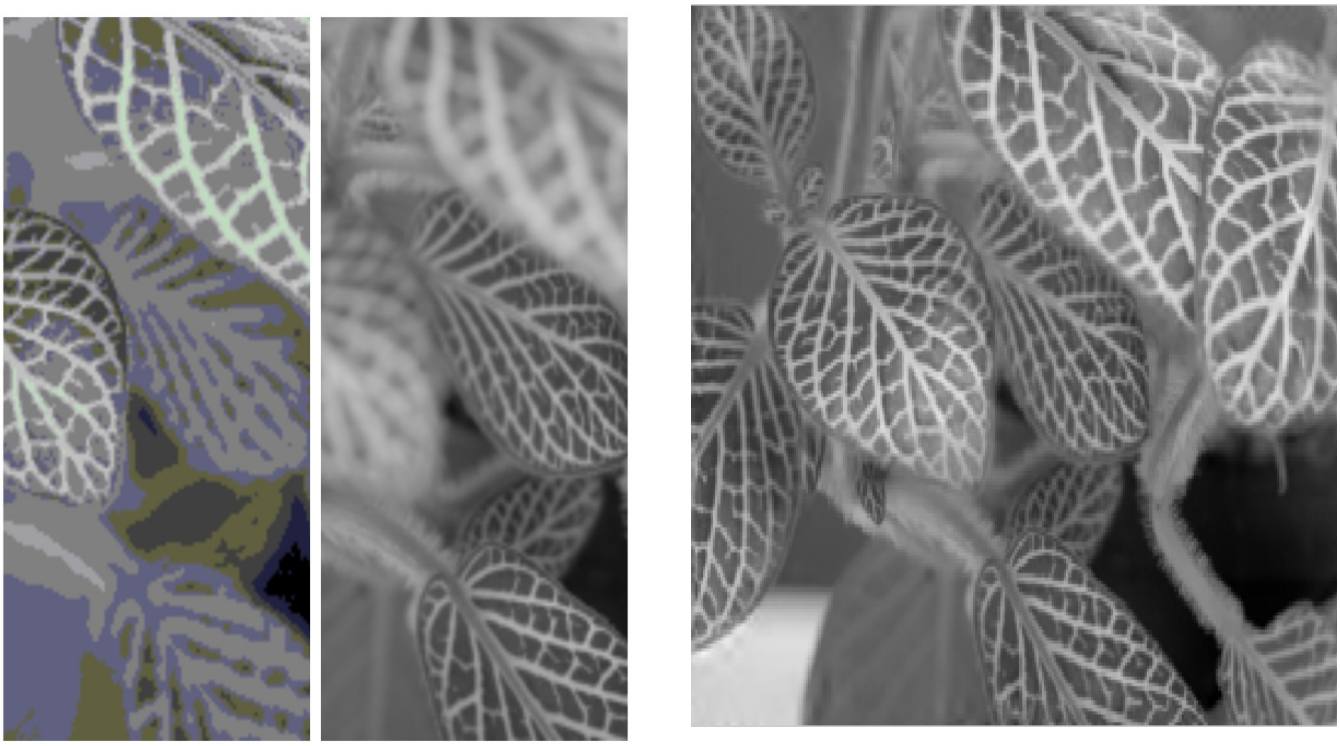

Input Images Output Fused Image

Figure 3.3.7: Example#7

Figure 3.3: Input Source Images and Fused Output Images For Algorithm 2

4. A TECHNIQUE OF IMAGE QUALITY ASSESSMENT

After fusing different images from different data sets, an efficient technique for image quality assessment is proposed. In this chapter, how the proposed technique utilizes the concept of using entropy to assess the quality of image in an appropriate way is shown. Results reveal that the proposed scheme is almost two times efficient and more accurate as compared to state of art existing techniques for image quality assessment. In order to propose the new technique, existing latest technique of image fusion based on the SSIM method along with the computation of three components luminance, contrast and structural similarity was analyzed to find out the failure and week points. After evaluating the glitches and failure cases of the existing technique, new technique was proposed to get the accurate quality measure of failure cases of the existing technique.

4.1. Existing Technique of Image Quality Measure for Fused Images

A useful approach is followed by the SSIM method is to see one patch of original image from three different facets including the luminance, contrast and structure. The easiest way to accomplish this is the decomposition of given patch of the image into three components:

$$a_k = \left|\left|a_k - \mu_{ak}\right|\right| . \frac{a_k - \mu_{ak}}{\left|\left|a_k - \mu_{ak}\right|\right|} + \mu_{ak} \qquad (4.1)$$

$$= \left|\left|\tilde{a}_k\right|\right| . \frac{\tilde{a}_k}{\left|\left|\tilde{a}_k\right|\right|} + \mu_{ak} \qquad (4.2)$$

$$= c_k . q_k + l_k \qquad (4.3)$$

In the above equation, $||.||$ represents the l^2 norm of the vector, μ_{ak} represents the mean value of patch, $\tilde{a}_k = a_k - \mu_{ak}$ is a mean-removed or zero-mean patch which holds information of contrast and structure. Scalar $l_k = \mu_{ak}$, $c_k = ||\tilde{a}_k||$ and the unit-length

vectors $q_k = \frac{\tilde{a}_k}{|}$ coarsely denote the luminance, contrast and the structure components ofa_k, correspondingly.

In MEF, straight conservancy of value of the luminance of patches of input source image (all of the patches of image are acquired with different situations like under and over exposed) is of little implication with apprehension to complete image quality; therefore it is excluded from the original patch assessment labeled below.

The perceptibility of local patch structure is mainly influenced by native contrast. The greater the value of the contrast will be will depict the enhanced perceptibility of the image. Whereas, the very high value of the contrast will cause the improbable description of local structure [64]. Assuming all patches of input source images as genuine acquiring of original scene, patch of the image with maximum value of contrast between all of images would relate to the finest perceptibility under realisticity constraint. Hence, the preferred contrast of fused image patch is achieved by maximum contrast of source image patches:

$$\hat{c} = \max c_k = \max \left|\tilde{a}_k\right| \qquad (4.4)$$

In above equation w (·) is representing the weighting function controls the impact of all patches of the input source image in the patch structure of the fused image. Instinctively, impact should rise with the high intensity of patch of image. A direct methodology that adapts the perception to apply the function of power weighting as mentioned below:

$$w\left(\tilde{a}_k\right) = ||\tilde{a}_k||^p \qquad (4.5)$$

In the above equation, p ≥ 0 is representing the exponent factor. Along with the numerous selections of values for p, this common construction will get to the weighting operations with diverse corporal implications. The higher value of p will represent the more stress on the image patches with comparatively greater power. Explicitly, p=0 means direct average value (in which low and high contrast patches for source images are responsible for

correspondingly); p=1 means the direction average value based on the length-weighted; p=2 relates to direction average based on energy-weighted; p=∞ means the selection of the direction compatible to the patch of the biggest vector length among all of the image patches. It's pending to find the value for p. Rather than setting the value of p as constant, the computerized scheme that selects the different values of p for corresponding spatial position robustly. The main objective is to regulate the comparative weighting elements in (4) centered on the uniformity among the structures of source image patches. For implementation, there is need to compute the constancy among the group of structural vectors$\{\tilde{a}_k\}$. Each vector points towards the specific direction in the vector space. In extreme situation, where a vector is the contrast enriched variation of other vector which shows that structural variations are no available among vectors and direction of both vectors will be similar. In the result, structure reliability measure among the group of vectors constructed at point of direction contract among them. In explicit, sturdier consistency among the group of vectors is computed as below:

$$R(\{\tilde{a}_k\}) = \frac{||\sum_{k=1}^{K} \tilde{a}_k||}{\sum_{k=1}^{K} ||\tilde{a}_k||} \qquad (4.6)$$

With triangular inequality, greater value of R and 0≤R≤1 specifies the stronger steadiness among the group of vectors. The sum of the group of the source patch vectors relates to joining the initial and lasts of these vectors in series, which produces the new vector $a' = \sum_{k=1}^{K} \tilde{a}_k||$ directing from origin point towards the culmination of the last patch vector. Length of this fresh vector a (shown as the numerator in Eq. (4.6)) is usually less than accumulating the length of the all patch vectors jointly (as shown in the denominator of Eq. (6)), however in case of all input source patch vectors directing towards precisely the similar path, these two methods are equivalent, directing the biggest probable value of (R=1).

In case of the R with small value, the compound input source patches provide the dissimilar structures with alike strength and as a result it becomes more appropriate to allot the identical

weights to them, by giving preference to the p with smallest value. On contrary, In case of the large value of R and alike structures of all source patches; strongest patch will ensure the highest contrast value and more resilient to the effect of image distortions and noise, and therefore it should be quantified with the greater weight, resultant to the high and required value of p. A practical method to calculate this is mentioned below:

$$p = \tan\frac{\pi R}{2} \qquad (4.7)$$

In the extreme cases, where all patches of source image approve with other pixels with the value of (R=1), and p=∞ is nominated, however in other case where there will be no constancy in the patch structures value of (R=0) and p=0 is chosen.

When value for p will be computed for all of the spatial locations, Eq. (4.4) is then executed to calculate $\hat{q}$, consequently joined with $\hat{c}$ in Eq. (5. 3) to produce the fresh vector.

$$\hat{x} = \hat{c}.\hat{q} \qquad (4.8)$$

After completely ensuing the complete structure of SSIM image quality assessment method [55],[56], SSIM index have been used in the propose scheme to assess the quality of fused images. The system illustration of the SSIM method is shown in figure 4.1.

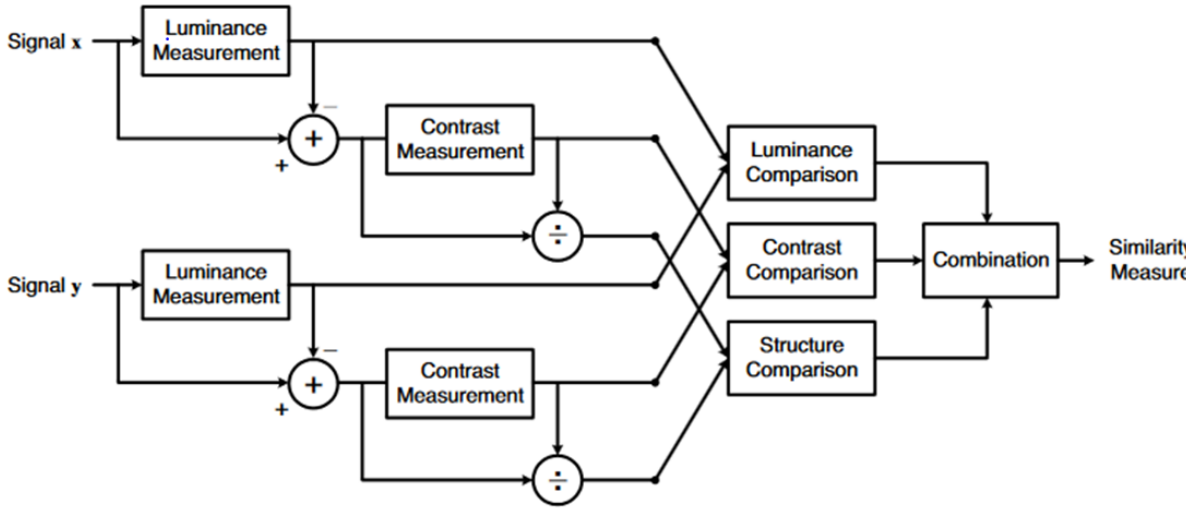

Figure 4.1: SSIM Image Quality Assessment Algorithm

Let's assume that a and b as positive image signals lined-up with each other like spatial patches excavated from each image. The purpose of this proposed scheme is to deliver a best approach to measure the quality of fused images. This measure can work as a quantitative calculation of quality of one image by assuming the second one to have superlative quality. In this case, both a and b is the continuous signals having the region of finite support, or either discrete signals represented as:

$$a = \{a_i | i = 1,2, \dots, S\} \; and \; b = \{b_i | i = 1,2, \dots, S\} \qquad (4.9)$$

Correspondingly, in the above equation, i is representing the sample index and S is representing the number of samples of signals (pixels).

This scheme segregates the mechanism of measurement of similarity into three different evaluations: contrast, luminance and structure. Initially, tvalue of luminance of all the image patches were compared. Supposing the discrete signals, assessed as value of the mean intensity:

$$\mu_a = \bar{a} = \frac{1}{S}\sum_{i=1}^{S} a_i \qquad (4.10)$$

The luminance comparison function l(a,b) is a function of μ_a and μ_b:

$$l(a,b) = l(\mu_a, \mu_b) \qquad (4.11)$$

In next stage, mean intensity from all of the image patches are removed. In the discrete system, the resultant signal a−μ_a relates with projection of the vector **a** in contrast to the hyperplane of:

$$\sum_{i=1}^{S} a_i = 0 \qquad (4.12)$$

Standard deviation is used as the approximation of the contrast of the given signal. A balanced calculation in the discrete form is calculated by:

$$\sigma_a = \left(\frac{1}{S-1} \sum_{i=1}^{S} (a_i - \mu_a)^2 \right)^{1/2} \qquad (4.13)$$

The comparison of contrast (a,b) becomes the comparison among $\sigma_a \; and \; \sigma_b$:

$$c(a,b) = c(\sigma_a \; and \; \sigma_b) \qquad (4.14)$$

The image patch is then normalized with the value of its own standard deviation, thus the two image patches that are in the comparison have unit standard deviation. Therefore, the structure comparison s(a,b) is directed on the normalized image patches as stated below:

$$s(a,b)=s\left(\frac{a-\mu_a}{\sigma_a}, \frac{b-\mu_b}{\sigma_b}\right) \qquad (4.15)$$

As a final point, these components are mutually pooled to prouced the one inclusive similarity evaluation:

$$S(a,b) = f(l(a,b), c(a,b), s(a,b) \qquad (4.16)$$

A significant point is that these components are comparatively autonomous from each other. Like, the variation in luminance has very minute influence on the image structure.

In order to complete this description of measure based on the similarity index stated above in Eq. (4.16), the three functions $l(a,b), c(a,b), s(a,b)$ and combination function f(.) needs to describe. These three similarity measures also need to fulfill the below mentioned conditions:

A. Symmetry

Symmetry is defined as:

$$S(a,b) = S(b,a) \qquad (4.17)$$

As the main determination is tho measurement of the similarity among the two images, by swapping the order number of the input source images does not disturb the measurement of output similarity.

B. Boundedness

Boundedness is a valuable feature for the similarity metrics as an upper bound could work as a sign to represnet the resemblence of the two images are to being perfectly same. This is opposite to the different existing techniques based on the signal-to-noise ratio that are usually unbounded. It can be defined as:

$$S(a,b) \leq 1 \qquad (4.18)$$

C. Unique maximum

The similarity evaluation should measure any differences existing amongthe orignal source images and fused image. The faultless score could be accomplished only in the case when the images being equated are precisely the same. It can be defined as:

$$S(a,b)=1 \qquad (4.19)$$

if a=b (in discrete depictions,$a_i = b_i \ for\ all\ i = 1,2, \ldots \ldots, N$

To compare the value of the luminance of the images:

$$S(a,b) = \frac{2\mu_a\mu_b + C_1}{\mu_a^2 + \mu_b^2 + C_1} \qquad (4.20)$$

In the above equation, constant C1 is incorporated to escape from unsteadiness when $\mu_x^2 + \mu_y^2$ is almost near to zero. Explicitly, constant C1 can be defined as:

$$C_{1=}(K_1L)^2 \qquad (4.21)$$

In the above equation, L is represnting the values of pixel with an active range of 8-bit grayscale image to 255 along with the value of K_1<<1, which is small constant. Similar contemplations were also used for the comparison of structure and contrast as represented in Eq. (4.20). It can be simply observed that the three properties stated ain the Eq. (4.20) are linked with Weber's law as well, used for luminance masking in human visual system. According to the Weber's law, the extent of the perceptible change in luminance ΔI is almost proportionate to the background value of luminance represented as I for the values of an

extensive range of luminance. HVS is delicate with the comparative change in luminance, but not in luminance. Supposing that the R denote the ratio of change in luminance comparative to the value of the background luminance, luminance of the slanted signal can be indicated as:

$$\mu_b = (1 + R)\mu_a \qquad (4.22)$$

Substituting the value of μ_b in Eq. (5.20:

$$l(a,b) = \frac{2(1+R)}{1 + (1+R)^2 + C_1/\mu_a^2} \qquad (4.23)$$

Supposing that constant C1 is sufficiently small as compare to the μ_a^2 and can unheeded, therefore l(a,b) is function of R as compare to the $\Delta I = \mu_b - \mu_a$. Subsequently, constant scheme is qualitatively trustworthy according to Weber's law. It delivers a quantitative estimation approach for situations in which variation in the luminance is quite larger as compare to threshold of visibility, that is beyoond the application limitations application of the Weber's law.

$$c(a,b) = \frac{2\sigma_a\sigma_b + C}{\sigma_a^2 + \sigma_b^2 + C} \qquad (4.24)$$

In the above equation, C_2 is a positive constant and is defined as:

$$C_2 = (K_2 L)^2 C_2 \qquad (4.25)$$

In the above equation, K_2 is satisfying the condition of K_2 << 1 and the quation is fullfilling the three properties mentioned above. A significant characteristic of this operation is the variation of equal amount of contrast $\Delta\sigma = \sigma_b - \sigma_a$, this calculation is very less subtle with condition of great ¾x base contrast as compare to low base contrast. It is accompanying with the features of contrast masking for HVS.

Contrast of the structure of images is directed subsequently the contrast normalization and luminance subtraction. Precisely, direction of the two unit vectors is assoociated as the

$\frac{(a-\mu_a)}{\sigma_a}$ and $\frac{(b-\mu_{yb})}{\sigma_b}$ both vectors are in hyperplane as defined by Eq. (4.12) with structures of images a and b. The correlation among both images a modest and effective assessment approach to measure the structural similarity amid two images. The correlation among $\frac{(a-\mu_a)}{\sigma_a}$ and $\frac{(b-\mu_b)}{\sigma_b}$ is same as coefficient of correlation among x and y. Therefore function of the structure comparison can defined as mentioned belwo:

$$s(a,b) = \frac{\sigma_{ab} + C_3}{\sigma_a \sigma_b + C_3} \qquad (4.26)$$

Since in the measuring values of luminance and contrast, a small constant was presented for both the denominator and numerator. In the discrete system, the value of σ_{ab} can be calculated as:

$$\sigma_{ab} = \frac{1}{S-1}\sum_{i=1}^{S}(a_i - \mu_a)(b_i - \mu_b) \qquad (4.27)$$

Symmetrically, coefficiant of correlation relates with the value of the angle cosine among the vectors $a - \mu_a$ and $b - \mu_b$ and s(a,b) can also be calculated for the non-positive values.

As a final point, comparison among three different Eqs. (4.20), (4.23) and (4.25) were combined as the subsequent similarity measure, the SSIM index between the images a and b:

$$SSIM(a,b) = [l(a,b)]^{\alpha}.[c(a,b)]^{\beta}.[s(a,b)]^{\gamma} \qquad (4.28)$$

In the above equation, parameters $\alpha > 0, \beta > 0 \; and \; \gamma > 0$ were used to control the comparative implication of mentioned components including the contrast, structure similarity and luminance. It is stress-free to say that this definition absolutely accomplishes the three conditions as mentioned above. Particularly these parameters were fixed as $\alpha = \beta = \gamma \; and \; C_3 = \frac{C_2}{2}$ This outputs in an obvious form of SSIM index as:

$$SSIM(a,b) = \frac{(2\mu_a\mu_b + C_1)(2\sigma_{ab} + C_2}{(\mu_a^2 + \mu_b^2 + C_1)(\sigma_a^2 + \sigma_b^2 + C_2)} \qquad (4.29)$$

Comparison of the local structure of Eq. (4.29) is implied by using the approach of sliding window on the complete image with the outcome of a quality map representing in what way

the structural information is mainatined at each spatial location. The quality map of fused image is then averaged to acquire the absolute value for the structural quality of the fused image:

$$Q(B) = \frac{1}{M}\sum_{j=1}^{M} S(\{A_k\}(j), b(j)) \qquad (4.30)$$

In above equation (4.30), j is representing the value of the spatial patch index, whereas M is total number of image patches.

Afterwards, a low-pass filter was iteratively applied by downsampling of the filtered images with factor value of 2. In the next stage, the original scale of image was indexed as the supreme scale value as 1, and the rougher scale as 0. The value of the Q should be in between 1 and 0.

After applying the iterations(1-1) as Scale l, the structure comparison at the l-th scale as shown in Eq. (4.29) was directed and indicated as $S_i(\hat{a}, b)$. After calculating the value of the structure comparsson at all scales, a group of multi-scale image quality maps were achieved. In the next step, quality map were combined at each scale by using the meaure mentioned in Eq. (4.30), a group of different quality scores with different scale-levels $\{Q_i(B)\}$ were achieved. At the end, the final metrics for the measurement of image quality was calculated with the combination of the different values of quality scores at different scale-levels with the same technique as stated in [57]:

$$Q(B) = \prod_{l=1}^{L} [Q_i(B)]^{\beta_l} \qquad (4.31)$$

In the above Eq.(4.31), L is represnting entire number of scales and β_l is weight allocated to l-th scale. This technique does not include any teaching procedure or introduction of any innovative parameter for quality assessment. All parameters mentioned in this technique are congenital from the earlier publications including the $C = (0.03D)^2$ [64] where D is

represnting the value of dynamic range of image intensity values which means the 8 bits/pixel gray-scale images, D=255 and L=3, and then the standardized weughts for the fine-to-coarse scale are mentioned as below:

$$\{\beta_1, \beta_2, \beta_3\} = \{1.071, 0.453, 0.476\} \qquad (4.32)$$

i. Results of Existing Technique of Image Quality Measure for Fused Images

In order to find the results of the existing technique of image quality assessment for fused images, different data sets of images were fused by using two different techniques of image fusion . After fusing the same images with two different algorithms of image fusion, two outputs were avail be to test the quality difference between them since for both algorithms same images were used. After applying the existing technique to number of data sets, few cases were found as failure cases of the existing technique by carefully observing the images quality with the human visual system. In these failure cases, the apparently good quality image was getting the low value of Q, whereas the poor quality image has received the high value of which should not be the case. The results of these failure cases will be clearly mentioned in Chapter 5 along with their values.

4.2. New Quality Assessment technique for Fused Images

After finding the failure cases of the existing technique, it was the new challenge to propose the new technique to find the value of the image score that should work fine for failure cases in the existing technique. By carefully analyzing the failue cases of the existing technique, it was found that the existing technique was giving the prefeerence to the image with the highest value of the contrast and then it was comparing all the other three componenents incluidng the luminnace, contrast and structural similarity component of the output fused image pixel by pixle with the source images. But the weak point in the existing scheme was that its not always necessary that the image with the highes value of contrast will be of good

quality as compare to the other images. Similarly, there is no doubt that comparing the output image with the input images used for fusion is the good approach to find out the similarity between the number of different input images of same scene with the output fused image is the good approach to find out the similarity index between the input and output image and then decide the image that has the more similarity with the input image will be of the good quality. But now here the question arises that does it always necessary that the image with more similarity with the input images will be a good one according to the quality. It can be also possible that the image contains noise and too much constraints that is destryin its quality but due to the high score of contrast and similarity index, it will be treated as the good one. Like, the problems found in the failure cases where the good image was having the low score of Q and the bad quality image was with high score of Q. In order to improve the results of this technique for the failure cases, various iterations and experiments have been made on the provided data sets.

After finding the scores for the quality matrix with existing technique of SSIM, it was found that there should be some mechanism that can be used to measure the score of the image quality with the content and data presnt in the image itself along with its comparison with the input images.

Entropy and depth is computed to measure the proposed efficeint quality matrix for fused images.

Proposed method is deliberated as a substitute to the currently available quality metrics for evaluation of the image quality of fused images. The perception of the amount of information entropy expresses that how much amount of randomness is present in the fused image; or it could be said as well that it represents the amount of the information present in the fused image. If uncertainty is measured before and after the fusion, reduction in uncertainty, i.e., entropy is quantitative amount of the information available in the fused image. Image quality

could be quantitatively linked with the transferred information represented by (T_a) existent in source images. As per the approach adopted in the physical measurement, the amount of information available in the image is directly linked with its quality, the high value of entropy will indicate the better image quality.

Exploration of the primarily directed towrads the introduction of the transmitted information as an quantity to assess the quality of image in 1970s. A technique of using the entropy for the measurement of quality assessment was offered for the radiographic images and then inferred this technique to calculate the quality of the tank-developed and automatic processor-developed images [58]. They exposed that quality of radiographic images is mostly affected by the number of structures and features like different exposure factors, characteristics of X-ray apparatus, system of intensifying screen-film and during the progression of film development. In case, all of mentioned factors having the same impact on quality of fused images are kept as constant by eliminating the practice of film development, performance of the development methods could be quantitatively estimated by connecting the quantity of information contributed by the tank-developed and automatic processor-established images. After this reserach journal, limited work by using the communicated information as a degree of image quality for image assessment has been indicated [59][60] whereas too much covenant of work on the mutual-information-based recording of multimodality and medical images with monomodality has been devoted since the early 1990s [61].

Provided events beginning from the E_1,..., E_n happening with the probabilities represnted as $p(E_1)$, ..., $p(E_n)$, average uncertainty linked with all of the mentioned events independently is indicated by using the Shannon entropy as:

$$H(E) = -\sum_{i=1}^{n} p(E_i).log_2 p(E_i) \qquad (4.33)$$

As *a* and *b* representing two random variables dependable on the variables of input and output, entropy measure for both the input and output are signified as *H*(*a*) and *H*(*b*), respectively. In the mentioned case, the joint entropy *H*(*a*, *b*) is demarcated as:

$$H(a,b) = H(a) + H_a(b) = H(b) + H_b(a) \qquad (4.34)$$

In the above Eq.(4.34), $H_a(b)\ and\ H_b(a)$ are representing conditional entropies which are infact the entropies of output in case where input is already known and similarly for input in case of already identified output, correspondingly. In this condition, T_a, *T*(*a*; *b*) can be calculated as:

$$T(a;b) = H(a) - H_b(a) = H(b) - H_b(a) \qquad (4.35)$$

$$H(a) = H(b) - H(a,b) \qquad (4.36)$$

With the help of an experiment wherein every input has an exclusive and the distinctive output connected among any one of different output sets. In this reserach work, for lenience, inputs may be deliberated as set of the subjects like phantoms in the variable of simplicity in configuration, nevertheless the outputs may be the dependable images variable in the optical density orgray level or an organized system initially acknowledged by Attneave [62]

Figure (4.2) displays the association in between the quantity of the comparative exposure and communicated information signified as *T* (*a*; *b*), for images with the two step blocks. The consequences are signifying that T (*a*; *b*) rises with the increase of the exposure aggregate. The surge in the value of *T* (*a*; *b*) is reflected due to the decrease in noise consequent from the increase of quantity of radiation. As exposed in Figure (4.3), value of the conditional entropy $H_a(b)$ decreases with the increase in the exposure. A previous study has quantified that $H_a(b)$ is rigorously related with noise of an imaging system [58].The less amount of level of noise level will depict the higher will amount of the exposure and less value of $H_a(b)$. Figure (4.4) is showing the root-mean-square noise. Figure 4.4 (a) and (b) illustrates the RMS value all wedges of A and B with all the steps as function of the exposure measure, correspondingly.

Average RMS values of dual-step wedges are delivered in the Figure 4.4 (c). It is deceptive from figures that RMS value diminutions with rise in exposure quantity. This outcome divulges the intellectual that $H_a(b)$ is linked with the noise available in the communication channel of information. Consequently, it becomes noticeable from the mentioned experimentations found that value of T_a and extent of the noise is meticulously connected.

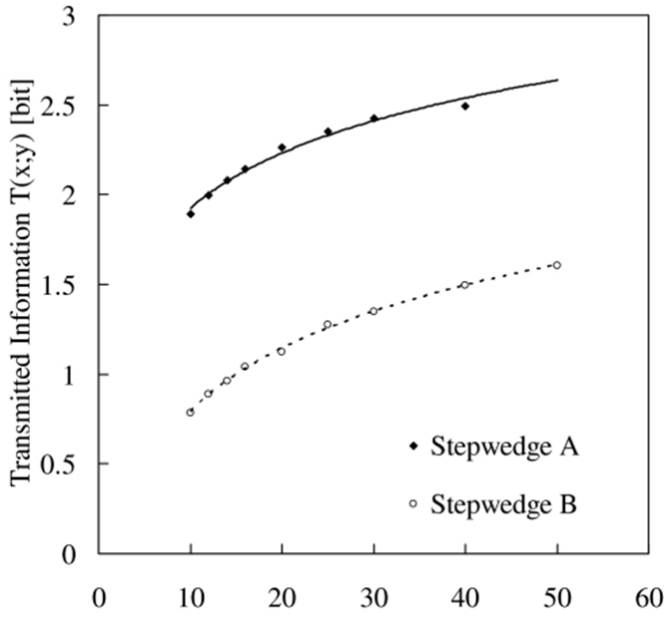

Figure 4.2: Relative Exposure Illustration

Communicated information $\boldsymbol{T}$ (a; $\boldsymbol{b}$) as an operation of the relative exposure quantity for images attained from the dual step wedges. For instance, values of T (a; b) at comparative exposure quantities with 20 and 30 for the step wedge A are 2.26 ± 0.01...

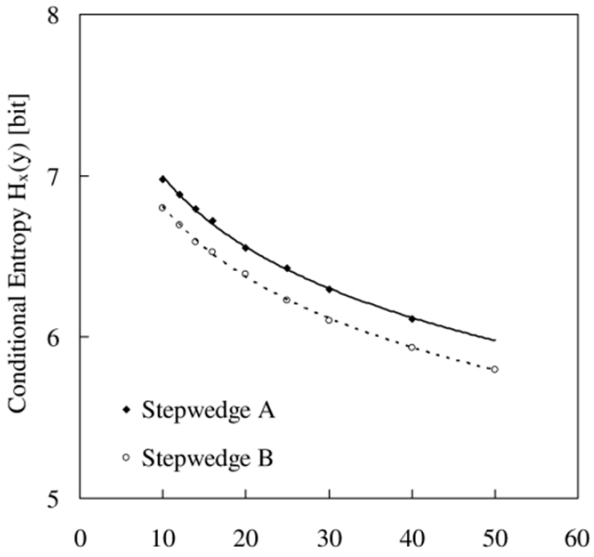

Figure 4.3: Relative Exposure Illustration

Conditional entropy $\boldsymbol{H}_a(\boldsymbol{b})$ as an operation function of the associated quantity of exposure for images acquired from the dual-step wedges. For instance, values of $\boldsymbol{H}_a(\boldsymbol{b})$ at associated quantity of exposure with values of 20 and 30 for the step wedge A are 6.55 ± 0.01 [bit] **...**

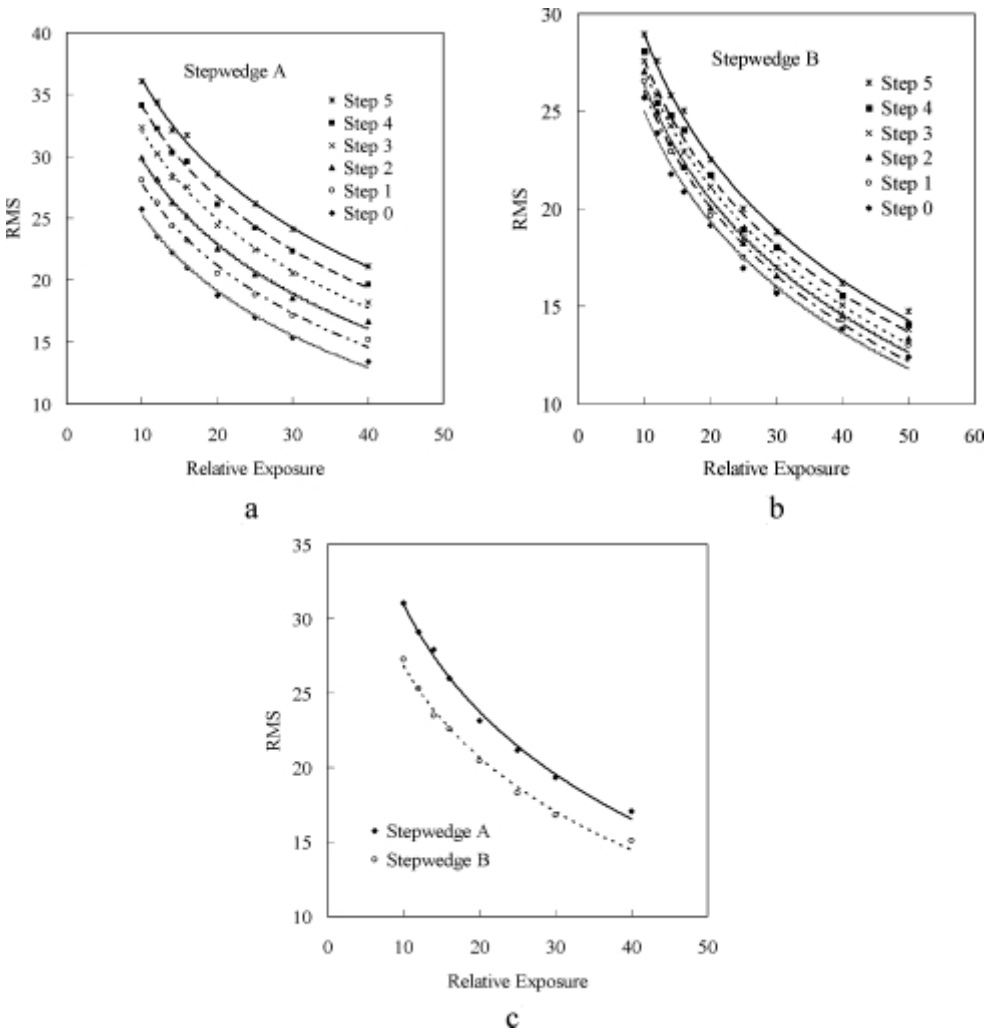

Figure 4.4: Relative Exposure

Root-mean-square noise as an operation function of the associated quantity of exposure for images acquired from dual-step wedges. Figure (4.4) (a) represents the RMS value for each step including the 0 to 5 of the step wedge A. Similarly figure (4.4) (b) represents the value of RMS for all steps including the 0 to 5 of the step wedge B, and figure (4.4) (c) is the average RMS value.

After finding the association of the computation of entropy with the image quality, a new scheme is proposed by using the existing algorithm of SSIM with three components of luminance, contrast and structural similarity and addition of entropy. All the association and calculation of the image entropy with its quality have been done and shown in the above

section. The new technique for image quality assessment is proposed by the computation of entropy of all the fused images as mentioned below:

Calculating the entropy as, mentioned in the equation (4.33):

$$H(I_a) = -\sum_{i=1}^{n} p(I_a).log_2 p(I_a) \qquad (4.37)$$

$$H(I_b) = -\sum_{i=1}^{n} p(I_b).log_2 p(I_b) \qquad (4.38)$$

In the above equations (4.37) and (4.38). I_a and I_b are the two fused images which have been fused by using the different techniques for image fusion as mentioned eralier.

$$Z_1 = mean\, H(I_a) \qquad (4.39)$$

$$Z_2 = mean\, H(I_b) \qquad (4.40)$$

In the above equations (4.39) and (4.40), $Z_1\ and\ Z_2$ is representing the mean values of the entroies calculated for image I_a and I_b.

After finding the entropies and the mean values of the entropies or all the provided data sets of images, the lowest and highes mean average value was taken for the approximation of the scaling of quality scale between 0 and 1.

$$\mathrm{R_1} = \mathrm{Z_1} - \frac{1.8799}{4.8022 - 1.8799} \qquad (4.41)$$

$$\mathrm{R_2} = \mathrm{Z_2} - \frac{1.8799}{4.8022 - 1.8799} \qquad (4.42)$$

In the above equations (4.41) and (4.42), $\mathrm{R_1 and\ R_2}$ are representing the approximations of the values of calculated entropies for image 1 and 2 to keep the scale of the image quality

score in between 0 and 1.

After finding the entropy of both the fused images, value of depth was found for both the fused images. Defocus approximation shows a significant part in numerous computer vision and graphics uses including the depth approximation, image quality calculation, image deblurring and relocating. Predictable approaches for defocus approximation have depend on the numerous images [90]. Value of depth is calculated by explicit or impicit deblurring process. The larger intensity of the images shows the larger value of depth.

Properly, the value of depth of the imag is found by using the below mentioned equation:

$$D = eTLe + \lambda(e- \hat{}e)TE(e- \hat{}e) \quad (4.43)$$

In the above equation, ˆe and e represents the vector systems of map of sparse defocus ˆ e(x) and the complete defocus map e(x) correspondingly. L is floor-covering Laplacian matrix and E is a diagonal matrix in which element Eii is 1 in case when pixel i is at edge site, and 0 else. The scalar λ equilibrium among the fidelity to sparse depth map and the smoothness of exclamation.

After computing the depth of images, depth and entropy was added with the already existing SSIM metrics with the below mentioned procedure.

$$U_1 = R_1 * \max\{(Q_1)(Q_2)\} \quad (4.44)$$

$$U_2 = R_2 * \max\{(Q_1)(Q_2)\} \quad (4.45)$$

In the above equations, Q_1 and Q_2 are represnting the image quality score calculated by the existing technique as mentioned above for image 1 and 2.

$$V_1 = Q_1 + U_1 \quad (4.46)$$

$$V_2 = Q_2 + U_2 \tag{4.47}$$

$$Q_2(new) = \frac{V_1 * Q_1}{D_1} \tag{4.48}$$

$$Q_2(new) = \frac{V_2 * Q_2}{D_2} \tag{4.49}$$

In the above equations (4.48) and (4.49) $Q_1(new)$ and $Q_2(new)$ are the new proposed image quality score for image 1 and 2.

The results of new proposed techniuqe and improvement in the failure cases of already existing techniques are presented in chapter 5.

Chapter 5

5. RESULTS

5.1. Results

In the proposed scheme, different data sets of images were taken and then fused by using the two different techniques for image fusion as mentioned in chapter 4. After fusing the data sets of images, the image quality of these images were evaluated by using the existing quality assessment technique and found 9 failure cases. Afterwards, new scheme was peoposed to improve the results of these failur cases and found the improved results as mentoned below:

Fused Image by First Technique of Image Fusion

Fused Image by Second Technique of Image Fusion

Figure 5.1.1: Example#1

Fused Image by First Technique of Image Fusion

Fused Image by Second Technique of Image Fusion

Figure 5.1.2: Example#2

Fused Image by First Technique of Image Fusion

Fused Image by Second Technique of Image Fusion

Figure 5.1.3: Example#3

Fused Image by First Technique of Image Fusion

Fused Image by Second Technique of Image Fusion

Figure 5.1.4: Example#4

Fused Image by First Technique of Image Fusion

Fused Image by Second Technique of Image Fusion

Figure 5.1.5: Example#5

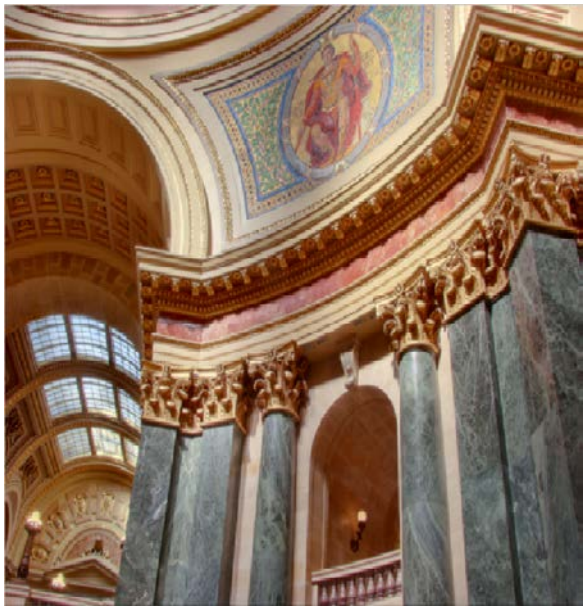

Fused Image by First Technique of Image Fusion

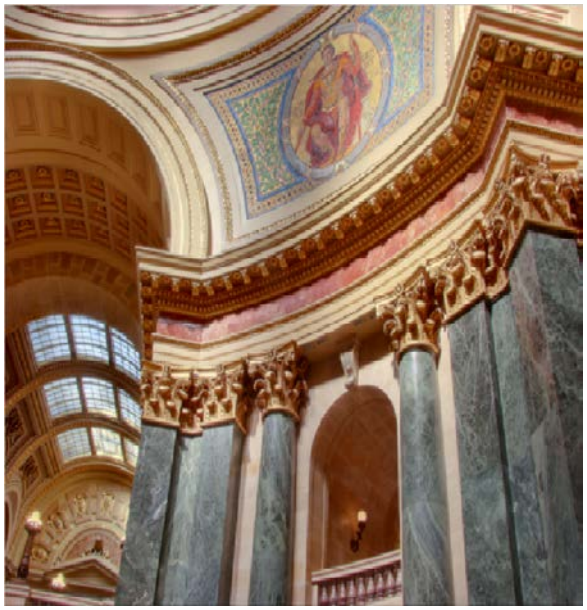

Fused Image by Second Technique of Image Fusion

Figure 5.1.6: Example#6

Fused Image by First Technique of Image Fusion

Fused Image by Second Technique of Image Fusion

Figure 5.1.7: Example#7

Figure 5.1: Failure Cases of Existing Image Quality Assessment: Fused Output Images with First and Second Technique of Image Fusion

In the above figure (5.1), the fused images for both the techniques are presented. These are the failure cases of the existing image quality assessment technique as the image with good quality has low score of Q and image with bad quality has the high value of Q as mentioned in the table (5.1).

Table 5.1: Comparison Between the Existing Technique for Image Quality Assessment

Data Sets of Images	Existing Q_1	New Q_1	Existing Q_2	New Q_2
Example#1	0.2911	0.144	0.2862	0.121
Example#2	0.144	0.043	0.1573	0.0350
Example#3	0.1210	0.036	0.1237	0.0319
Example#4	0.1525	0.058	0.1750	.0484
Example#5	0.4844	0.482	0.5257	0.394
Example#6	0.0706	0.014	0.0783	0.013
Example#7	0.0747	0.0177	0.1038	0.0103

In the figure 5.1 and table 5.1, it can be easily seen that for the existing algorithm the image with good perceptual quality has low score of Q and in the comparison image with bad quality has high score of Q which is the failure case of the existing algorithm. In table 5.1, the values of Q the image quality score for new proposed scheme can be seen in which image with good quality has the high value of Q and vice versa except the Belgium house data set. For Belgium house data set, values of entropies for both the images were quite same and as a result the Q score of bad image is greater in value of 0.002 than the good image. This minor difference in accuracy can be ignored. However, results for all the other images are improved as compare to the existing algorithm.

Chapter 6

6. FUTURE WORK

In this thesis, a new scheme for image quality assessment was proposed with the results having the improvements in the existing technique of image quality assessment. The proposed scheme incorporates the already existing SSIM technique along with the three components including the luminance, contrast and structure similarity with the entropy of the image in order to improve the failure and week points of the existing algorithm. The results of the new proposed scheme were achieved successfully and presented above. However, there is still room for the improvement. Since, as mentioned below one case of image data set named Belgium House was still not giving the desired results with the proposed scheme. Therefore, further improvements in the image quality assessment can be done as a future work.

For future work, below mentioned are few recommendations:

- More features of the images can be added in the quality assessment technique like depth or focus of the image in order to improve the accuracy of the results.
- An automated fusion algorithm can be designed along with the quality assessment technique that automatically generates the best outcome of the captured photos instantly.

REFERENCES

[1] S. Xydeas and V. S. Petrovic, "Objective pixel-level image fusion performance measure," Proc. SPIE, Sensor Fusion, Archit., Algorithms, Appl. IV, vol. 4051, pp. 89–98, April 2000

[2] P.-W. Wang and B. Liu, "A novel image fusion metric based on multi-scale analysis," Proc. IEEE 9th Int. Conf. Signal Process, pp. 965–968, October 2008.

[3] Y. Zheng, E. A. Essock, B. C. Hansen, and A. M. Haun, "A new metric based on extended spatial frequency and its application to DWT based fusion algorithms," Inf. Fusion, vol. 8, no. 2, pp. 177–192, 2007

[4] G. Piella and H. Heijmans, "A new quality metric for image fusion," Proc. IEEE Int. Conf. Image Process., vol. 3.,pp. III-173–III-176, September 2003.

[5] N. Cvejic, A. Loza, D. Bull, and N. Canagarajah, "A similarity metric for assessment of image fusion algorithms," Int. J. Signal Process.,vol.2,no. 3, pp. 178–182, 2005.

[6] C. Yang, J.Q. Zhang, X.R. Wang, and X. Liu, "A novel similarity based quality metric for image fusion,"Inf. Fusion, vol. 9, no. 2, pp. 156–160,2008

[7] M. Hossny, S. Nahavandi, and D. Creighton, "Comments on 'information measure for performance of image fusion," Electron. Lett., vol. 44, no. 18, pp. 1066–1067, August 2008

[8] N. Cvejic, C. N. Canagarajah, and D. R. Bull, "Image fusion metric based on mutual information and Tsallis entropy,"Electron. Lett.,vol. 42, no. 11, pp. 626–627, 2006.

[9] S. Sonawane and A.M. Deshpande, "Image Quality Assessment Techniques: An Overview," JERT, vol.3, no.4, 2014.

[10] Nisha and S. Kumar, "International Journal of Advanced Research in Computer Science and Software Engineering," IJARCSSE, vol.3, no.7,pp. 636-640, 2013.

[11] "Methodology for the Subjective Assessment of the Quality of Television Pictures", Recommendation ITU-R Rec. BT.500- 11.

[12] S.Patil and S. Sheelvant, "Survey on Image Quality Assessment Techniques," IJSR, vol.4, no.7, pp. 1757-1759, July 2015.

[13] H.A.Vittal and P. Jagalingam, "A Review of Quality Metrics for Fused Image," ScienceDirect, vol.4, pp.133-142, 2015.

[14] Q. Du, N. H. Younan, R. King and V. P. Shah, "On the Performance Evaluation of Pan-Sharpening Techniques," IEEE Geoscience and Remote Sensing Letters, Vol. 4, No. 4, pp. 518-522, 2007.

[15] L. Atidel, E. Viennet and A. Beghdadi, “Combining and Selecting Indicators for Image Quality Assessment,” Proceedings of the ITI 2009 31st Int. Conf. on Information Technology Interfaces, 2009,

[16] G.G.Anna and P.A. Kethsey, “A Survey On Different Approaches Used In Image Quality Assessment,” IJETAE, vol.3, no.2, pp. 197-203, February 2013

[17] J. Caviedes and S. Gurbuz, “No-reference sharpness metric based on local edge kurtosis,” Proceedings of IEEE International Conference on Image Processing,vol. 3, pp. 53–56, 2002.

[18] A.Ciancio, A. D. Costa, E.D.Silva, A. Said, R. Samadani, P. Obrador, “No-Reference Blur Assessment of Digital Pictures Based on Multifeature Classifiers,” IEEE Transaction on Image Processing, vol.20, no.1, 64-75, 2011.

[19] B. Margaret, “IEEE P1858 CPIQ Overview,” IEEE Standards Association, 2016.

[20] Q. Li and Z. Wang, “Reduced-reference image quality assessment using divisive normalization-based image representation,” IEEE J. Sel. Topics Signal Process., vol. 3, no. 2, pp. 202–211, April 2009.

[21] S. Michele, A.C. Bovik and C. Charrier, “A DCT Statistics-Based Blind Image Quality,” IEEE, IEEE Signal Processing Letters, Institute of Electrical and Electronics Engineers, vol. 17, no. 6, June 2010

[22] H.R. Sheikh, M.F. Sabir and A.C. Bovik, "A statistical evaluation of recent full reference image quality assessment algorithms", *IEEE Transactions on Image Processing*,vol. 15, no. 11, pp. 3440-3451, Nov. 2006

[23] N. Ponomarenko, C. Carli, V. Lukin, K. Egiazarian, J. Astola and F. Battisti, "Color Image Database for Evaluation of Image Quality Metrics", Proceedings of International Workshop on Multimedia Signal Processing , vol.5, no.16, pp. 403-408, 2008

[24] J. Redi, H. Liub, H. Alersb, R. Zuninoa, and I. He, “Comparing Subjective Image Quality Measurement Methods for the Creation of Public Databases,” Proceedings of SPIE-IS&T Electronic Imaging, vol. 7529, 2010.[doi: 10.1117/12.839195].

[25] D.M. Rouse, R. Pepion, P. L. Callett, and S.S. Hemami, “Tradeoffs in Subjective Testing Methods for Image and Video Quality Assessment,” Proceedings of SPIE - The International Society for Optical Engineering, vol. 75270, 2010. [10.1117/12.845389].

[26] A. Lahouhou, E. Viennet and A. Beghdadi, “ Selecting Low-level Features for Image Quality Assessment,” Statistical MethodsJournal of Computing and InformationTechnology, vol. 18, 2010.

[27] R., K. Mantiuk, A. Tomaszewska, and R. Mantiuk, “Comparison of four subjective methods for image quality assessment,” Computer Graphics Forum, 2012

[28] Z.Wang, A. C. Bovik, H. R. Sheikh, and E. P. Simoncelli, “Image quality assessment: from error visibility to structural similarity,” IEEE Transactions of Image Process, vol. 13, no. 4, pp. 600–612, 2004.

[29] A. M. Eskicioglu, P. S. Fisher, “Image Quality Measures and Their Performance” IEEE Transactions on Communication, vol. 43, no. 12, pp. 2959-2965, December 1995.

[30] S.S.Bedi, A.Jyoti and A.Pankaj, “Image Fusion Techniques and Quality Assessment Parameters for Clinical Diagnosis: A Review,” IJARCCE, vol.2, no.2, pp.1153-1157, February 2013

[31] Z.Wang, A.C. Bovik, “A universal image quality index,” IEEE Processing Letters, vol. 9, pp. 81–84, March 2002.

[32] Z. Wang, A. C. Bovik, H. R. Sheikh, and E. P Simoncelli, “Image quality assessment: From error visibility to structural similarity,” IEEE Transactions of Image Processing, vol. 13, no. 4, pp. 600–612, 2004.

[33] S.K.Sweta and D.U.Shah, “A Review on Image Fusion Techniques,” IJIREEICE, vol.2, no.3, pp.1258-1261, March 2014.

[34] S.Bhargavi and C. Pavithra, “Fusion of two Images based on Wavelet Transform”, Internatioal Journal of Innovative Research in Science, Engineering and Technology, vol. 2, no. 5, May 2013.

[35] S., and V. Rajinder, “Review of image fusion techniques,” IRJET, vol.2, no.3, pp.333-339, June 2015.

[36] H.B. Kekre, M. Dhirendra and S. Rakhee, “Review on image fusion techniques and performance evaluation parameter,” IJEST, vol.5, no.4, pp. 880-889, April 2013.

[37] D. Jiang, D. Zhuang, Y. Huang and J. Fu, “Survey of Multispectral Image Fusion Techniques in Remote Sensing Applications, Image Fusion and Its Applications,” InTech, 2011. [DOI: 10.5772/10548].

[38] C.Pohl and J.L.V. Genderen, “Multisensor image fusion in remote sensing: Concepts, methods and applications,” International Journal of Remote Sensing, vol. 19, pp. 823-854, 1998.

[39] R. Sivagami, V. Vaithiyanathan, V. Sangeetha, A .Ifjaz, K. J. A. Sundar and K. D.Lakshmi, “Review of Image Fusion Techniques and Evaluation Metrics for Remote Sensing Applications,” vol. 8, no.35, December 2015.

[40] D.Sahu, M.Parsai, “Different Image Fusion Techniques-A Critical Review”, International Journal of Modern Engineering Research, vol.2, October 2012.

[41] K.Rani,R.Sharma, “Study of Different Fusion Algorithm”,International journal of Emerging Technology and advanced Engineering , vol.3, May 2013.

[42] M. Li and Y. Dong, “Review on technology of pixel-level image fusion.” IEEE: International Conference on Measurement, Information and Control (ICMIC), vol. 1, 2013.

[43] J. Dong, D. Zhuang, Y. Huang, J.Fu, “Survey of Multispectral Image Fusion Techniques in Remote Sensing Applications,” Image Fusion and Its Applications in techonology, pp.1–22, 2011.

[44] A. Sasi, L. Parameswaran, S. Sruthy, “Image Fusion technique using DT-CWT, Automation, Computing, Communication, Control and Compressed Sensing,” International Multi-conference on (iMac4s), pp.160-164, March 2013

[45] K.Rani, R.Sharma, “Study of Different Fusion Algorithm”, International journal of Emerging Technology and advanced Engineering , vol.3, May 2013.

[46] R.Desale, S.Verma, “Study and Analysis of PCA,DCT & DWT based Image Fusion Techniques,” International Conference on Signal processing, Image Processing and Pattern Recognition, 2013.

[47] J. kaur and E. R. S. Boparai. “An evaluation on different image fusion techniques” IPASJ International Journal of Computer Science (IIJCS), vol. 2, no. 4, April 2014.

[48] H. Zhang and X. Cao. “A way of image fusion based on wavelet transform,” 9th International Conference on Mobile Ad-hoc and Sensor Networks, IEEE, 2013.

[49] K. Sascha and E. Manfred, “Performance of evaluation methods in image fusion,” 12th International Conference on Information Fusion, pp. 1409-1416, July 2009.

[50] W.A. Hallada, and S. Cox, “Image sharpening for mixed spatial and spectral resolution satellite systems,” Proceedings of the 17th International Symposium on Remote Sensing of Environment, pp.1023–1032, 1983.

[51] Y. Siddiqui, “The modified IHS method for fusing satellite imagery,” ASPR Annual Conference Proceedings, Anchorage, Alaska, 2003.

[52] L.Yu, L. Shuping and W.Zengfu, “A General Framework for Image Fusion Based on Multi-scale Transform and Sparse Representation,” Preprint submitted to Information Fusion, September 2014

[53] G. Piella, “A general framework for multiresolution image fusion: from pixels to regions,” Information Fusion, vol.4, no. 4, pp. 259–280, 2003.

[54] B. A. Olshausen, D. J. Field, “Emergence of simple-cell receptive field properties by learning a sparse code for natural images,” vol. 381, no.6583, pp. 607–609, 1996.

[55] W. Zhou, B.C.Alan and S.R.Hamid, “Structural Similarity Based Image Quality Assessment,” Chapter in Digital image quality and perceptual coding (H.R.Wu and K.R.Rao,eds,), Marcel Dekker series in Signal processing and Communication, November 2015

[56] W. Zhou, B.C.Alan, S.R.Hamid and S.P.Eero, “Image Quality Assessment: From Error Visibility to Structural Similarity,” IEEE trans. of Image fusion, vol.13, no.4, pp.600-612, April 2004

[57] Z. Wang, E. P. Simoncelli, and A. C. Bovik, “Multiscale structural similarity for image quality assessment,” in Proceedings of 37th IEEE Asilomar Conference of Signals and Systems and Computing, vol. 2, pp. 1398–1402, November 2003.

[58] S.Uchida and D. Tsai, “Evaluation of radiographic images by entropy: Application to development process,” Applied Physics, vol.17, pp.17:2029–2034, 1978. [doi: 10.1143/JJAP.17.2029].

[59] S.Uchida and D. Tsai, “Reliability of the modulation transfer function of radiographic screen-film system measured by the slit method,” Applied Physics, vol.18, pp.1571–1574, 1979. [doi: 10.1143/JJAP.18.1571].

[60] S. Uchida and H.Fujita, “Assessment of radiographic granularity by a single number,” Jpn J Appl Physics, vol.19, pp.1403–1410, 1980. [doi: 10.1143/JJAP.19.1403].

[61] B.Kim, J. Boes and K. Frey, “Mutual information for automated unwarping of rate brain autoradiograph,” Neuroimage. vol.5, pp.31-40, 1997. [doi: 10.1006/nimg.1996.0251].

[62] M. Choi, “A New Intensity-Hue-Saturation Fusion Approach to Image Fusion With a Tradeoff Parameter,” IEEE Transactions on Geoscience And Remote Sensing, vol. 44, no. 6, pp. 1672-1682, June 2006.

[63] A.H. Muhammad, S.M. Syed and I. Muhammad, “Wavelet Based Multi-Focus Image Fusion using Adaptive Sized Blocks,” IEEE, 2009

[64] M.Keda, Z.Kai and W.Zhou, " Perceptual quality assessment for multi-exposure image fusion,” IEEE, Transactions of Image Processing, vol.24, no.11, 2015.

[65] M. N. Do and M. Vetterli, “The Contourlet Transform: An Efficient Directional Multiresolution Image Representation” IEEE Transactions on Image Processing, vol.14, no.12, pp.515-519, November 2005.

[66] S. Winkler, “Video Quality,” Digital Video Quality, West Sussex, England: Wiley, pp.35-70, 2005.

[67] M. Shahid, A. Rossholm, and B. Lövström, “A no-reference machine learning based video quality predictor”, IEEE 5th International Workshop on Quality of Multimedia Experience, pp. 176 –181, October 2013.

[68] Z. Wang, A. C. Bovik, and L. Lu, “Why is image quality assessment so difficult?,” Acoustics, Speech, and Signal Processing (ICASSP), IEEE International Conference on, vol. 4, pp. IV–3313, 2002.

[69] M. Saad, A. Bovik, and C. Charrier, “A dct statistics-based blind image quality index,” Signal Processing Letters, IEEE, vol. 17, no. 6, pp. 583–586, 2010.

[70] M. Saad, A. Bovik, and C. Charrier, “Dct statistics model-based blind image quality assessment,” Image Processing (ICIP), 18th IEEE International Conference , pp. 3093–3096, 2011.

[71] A. Moorthy and A. Bovik, “A two-step framework for constructing blind image quality indices,” Signal Processing Letters, IEEE, vol. 17, no. 5, pp. 513–516, 2010.

[72] A. Moorthy and A. Bovik, “Blind image quality assessment: From natural scene statistics to perceptual quality,” Image Processing, IEEE Transactions , vol. 20, no. 12, pp. 3350–3364, 2011.

[73] P. Ye and D. Doermann, “No-reference image quality assessment using visual codebooks,” Image Processing, IEEE Transactions , vol. 21, no. 7, pp. 3129–3138, 2012.

[74] Z. Wang and A.C. Bovik, “Mean squared error: love it or leave it? a new look at signal fidelity measures,” Signal Processing Magazine, IEEE, vol. 26, no.1, pp.98–117, 2009

[75] T.-J. Liu, W. Lin, and C.-C. J. Kuo, “Recent developments and future trends in visual quality assessment,” Proceedings of APSIPA ASC, pp. 1–10, October 2011.

[76] Z. Wang and A. Bovik, “Mean Squared Error: Love It or Leave It?,”IEEE Signal Processing Magazine, pp. 98–117, January 2009.

[77] K. Egiazarian, J. Astola, N. Ponomarenko, V. Lukin, F. Battisti and M. Carli, “New full-reference quality metrics based on HVS,” Proceedings of the Second International Workshop on Video Processing and Quality Metrics, Scottsdale, 2006.

[78] D.M. Chandler, and S. S. Hemami, “VSNR: A Wavelet-Based Visual Signal-to-Noise Ratio for Natural Images,” IEEE Transactions on Image Processing, vol. 16 , no.9, pp. 2284-2298, 2007.

[79] Z. Wang and E.P. Simoncelli, “Translation insensitive image similarity in complex wavelet domain,” in Proceedings of IEEE International Conference of Acoustics, Speech, Signal Processing, pp. 573–576, March 2005.

[80] L. Zhang, L. Zhang, X. Mou, and D. Zhang, “FSIM: A feature similarity index for image quality assessment,” to appear, IEEE Transactions on Image Processing, 2011

[81] H. Yogita and H.Y.Patil, “A survey on image quality assessment techniques, challenges and databases,” International Journal of Computer Applications, 2015.

[82] H. Luo, “A training-based no-reference image quality assessment algorithm,” in Proceedings of IEEE International Conference of Image Processing, pp. 2973–2976, October 2004

[83] T.J. Liu, W. Lin, and C.C. J. Kuo, “Image quality assessment using multi-method fusion,” IEEE Transactions of Image Processing, vol. 22, no. 5, pp. 1793–1807, May 2013.

[84] S. Suresh, V. Babu, and N. Sundararajan, “Image quality measurement using sparse extreme learning machine classifier,” Proceedings of IEEE 9th International Conference of Control, Automation, Robotic Visuals, pp. 1-6, December 2006.

[85] S. Suresh, V. Babu, and H. J. Kim, “No-reference image quality assessment using modified extreme learning machine classifier,” Journal of Applications of Soft Computing, vol. 9, no. 2, pp. 541–552, March 2009.

[86] M. Narwaria and W. Lin, “Objective image quality assessment based on support vector regression,” IEEE Transactions of Neural Networks, vol. 21, no. 3, pp. 515–519, March 2010.

[87] L. Jin, S. Cho, T.J. Liu, K. Egiazarian, and C.C. J. Kuo, “Performance comparison of decision fusion strategies in BMMF-based image quality assessment,” Proceedings of Asia-Pacific Signal Information Processing Association Annual Submission Conference (APSIPA ASC), Hollywood, CA, USA, pp. 1-4, December 2012.

[88] L. Zhang, L. Zhang, X. Mou and D. Zhang, “ FSIM: A feature similarity index for image quality assessment,” *Image Processing, IEEE Transactions, vol.20, no.8, pp.* 2378–2386, 2011.

[89] L., T. Jung, K. Hsien & Lin, J. Y.Chieh , L., Weisi, K. and C.C. Jay, “ A ParaBoost Method to Image Quality Assessment,” IEEE transactions on neural networks and learning systems, 2015. [28. 10.1109/TNNLS.2015.2500268].

[90] Z.Shaojie, S.Terence, “Defocus Map Estimation From a Single Image,” Patter Recognition, March 2011.